IEEE Access
Multidisciplinary | Rapid Review | Open Access Journal

Received 12 September 2022, accepted 26 September 2022, date of publication 3 October 2022, date of current version 13 October 2022.

Digital Object Identifier 10.1109/ACCESS.2022.3211504

RESEARCH ARTICLE

Design of Soccer League Optimization Based Hybrid Controller for Solar-Battery Integrated UPQC

KOGANTI SRILAKSHMI[1], NAKKA SRINIVAS[2], PRAVEEN KUMAR BALACHANDRAN[2], (Senior Member, IEEE), JONNALA GANESH PRASAD REDDY[3], SRAVANTHY GADDAMEEDHI[1], NAGARAJU VALLURI[4], AND SHITHARTH SELVARAJAN[5], (Senior Member, IEEE)

[1]Department of Electrical and Electronics Engineering, Sreenidhi Institute of Science and Technology, Hyderabad, Telangana 501301, India
[2]Department of Electrical and Electronics Engineering, Vardhaman College of Engineering, Hyderabad, Telangana 501218, India
[3]Department of Electrical and Electronics Engineering, Sree Vahini Institute of Science and Technology, Tirvuru, Andhra Pradesh 521235, India
[4]Department of Electronics and Communication Engineering, Sreenidhi Institute of Science and Technology, Hyderabad, Telangana 501301, India
[5]Department of Computer Science and Engineering, Kebri Dehar University, Somali 001, Ethiopia

Corresponding author: Shitharth Selvarajan (shitharth.s@ieee.org)

ABSTRACT Nowadays, integration of renewable energy source like solar, wind etc in the grid is encouraged to reduce the losses and meet the demand. However, the integration of these renewable sources, power electronic devices, non-linear and un-balanced loads leads to the power quality issues this motivated power researchers for the development of new controllers and techniques. This paper develops a soccer-league algorithm based optimal tuned hybrid controller for the unified power quality conditioner associated with the solar power and battery-storage systems with the Boost converter and Buck Boost converter. The UPQC simultaneously performs both the functions of Shunt active power filter and series active power filter. The proposed optimally designed controller adapts both the properties of fuzzy logic-controller and SOL algorithm tuned proportional-integral controllers. The K_p, K_i values of shunt and series controllers are treated as control variables, which are optimally tuned by SOL to satisfy the objective function. The key contributions of the proposed work are the reduction of total harmonics in current waveforms thereby enhancing the power factor, quick action to maintain the constant DC-Link capacitor voltage during the solar irradiation variations, elimination of voltage sag/swell/ large disturbance, and appropriate compensation for the un-balanced networks and loads. The performance investigation of SLOHC was carried-out with four test studies for different combinations of unbalanced/balanced loads and supply voltage of 3-phase distribution network. Comparative analysis was carried out with those of standard methods like a genetic algorithm, biogeography-based optimization, and proportional-integral controllers. The proposed method reduces the total harmonic distortion to 2.06%, 2.44%, 2.40%, and 2.32% which are much lower than those of existing methods available in literature. The design has been performed on MATLAB/simulink software.

INDEX TERMS Power quality, soccer league optimization, UPQC, fuzzy logic, PI-C, battery storage system, solar PV system.

NOMENCLATURE

UPQC	Unified Power Quality Conditioner.
SLOHC	Soccer league optimization based hybrid controller.
SOL	Soccer league optimization.
BBO	Biogeography-based optimization.
GA	Genetic algorithm.
U-PVBS	Solar battery integrated UPQC.
SHAPF	Shunt active power filter.
SAPF	Series active power filter.
PQ	Power quality.

The associate editor coordinating the review of this manuscript and approving it for publication was Wai-Keung Fung.

SP	Solar Photo-Voltaic system.
BS	Battery Storage.
FL-C	Fuzzy Logic Controller.
PI-C	Proportional Integral.
SM-C	Sliding-mode Control.
ANN-C	Artificial neural network controller.
PWM	Pulse width modulation.
THD	Total harmonic distortion.
VSC	Voltage source converter.
PLL	Phase-Locked-Loop.
LPF	Low Pass Filters.
PF	Power Factor.
$V_{S\_a}, V_{S\_b}, V_{S\_c}$	Source voltage for abc phases.
$i_{S\_a}, i_{S\_b}, i_{S\_c}$	Source current for abc phases.
R_S	Source Resistance.
L_S	Source Inductance.
$V_{l\_a}, V_{l\_b}, V_{l\_c}$	Load voltage for phases a, b, c.
V_{S_d}, V_{S_q}	Source voltage in d-q domain.
$V_{se\_a}, V_{se\_b}, V_{se\_c}$	Series injected voltage for phases a, b, c.
$V_{l\_a}^{ref}, V_{l\_b}^{ref}, V_{l\_c}^{ref}$	Reference load voltages for phases a, b, c.
$V_{se\_a}^{ref}, V_{se\_b}^{ref}, V_{se\_c}^{ref}$	Series injected reference voltage for phases a, b, c.
$V_{l\_d}^{ref}, V_{l\_q}^{ref}$	Reference load voltage in d-q domain.
V_{l_d}, V_{l_q}	Load voltage in d-q domain.
$V_{S\_d}^{ref}, V_{S\_q}^{ref}$	Reference source voltage in d-q domain.
$i_{l\_a}, i_{l\_b}, i_{l\_c}$	Load current for phase a, b, c.
i_{l_d}, i_{l_q}	Load current in d-q domains.
$i_{sh\_a}, i_{sh\_b}, i_{sh\_c}$	SHAPF injected current for phases a, b, c.
$i_{sh\_a}^{ref}, i_{sh\_b}^{ref}, i_{sh\_c}^{ref}$	Reference SHAPF injected current for phases abc.
$i_{sh\_a}, i_{sh\_b}, i_{sh\_c}$	SHAPF injected current for abc phases.
C_{sh}	SHAPF Capacitance.
R_{sh}	SHAPF Resistance.
L_{sh}	SHAPF Inductance.
K_{i_sh}	Integral gain of SHAPF.
K_{p_sh}	Proportional grain of SHAPF.
$K_{i\_se\_d}$	Integral gain of SAPF in d domain.
$K_{p\_se\_d}$	Proportional grain of SAPF in d domain.
$K_{i\_se\_q}$	Integral gain of SAPF in q domain.
$K_{p\_se\_q}$	Proportional grain of SAPF in q domain.
C_{dc}	Capacitance of the capacitor across DC-Link.
V_{dc}	Actual voltage of DC-Link capacitor.
V_{dc}^{ref}	Reference voltage of DC-Link capacitor.
Δi_{dc}	DC-Link output error.
P_{PV}	Solar PV output power.
V_{PV}	Solar output voltage.
I_{PV}	Solar output current.
$P_{DC-Link}$	Power at DC-Link.
P_{BS}	Battery Power.
V_{BS}	Battery voltage.
i_{BS}	Battery current.
Q	Battery capacity.
MF	Membership Functions.
E	Error.
CE	Change in error.
BC	Boost Converter.
BBC	Buck-Boost Converter.
SOC	State of charge of Battery.
SPG	Solar Power Generated.

I. INTRODUCTION

The Distribution network is prone to huge PQ problems when compared to the Generation/ Transmission. The deterioration of PQ refers to the quality of voltage and currents like harmonics, PF, voltage sag/ swell/ large disturbance, interruptions, flickers, etc., mainly due to the integration of renewable energy sources, ever-growing usage of power electronic devices and unbalanced nonlinear loads.

A. CHALLENGES AND MOTIVATION

The increase in application of large non-linear industrial load has led to increase in harmonic currents thereby reducing PF. Electricity with a bad quality is dangerous and uneconomical at both utility and consumer end. Therefore, maintain of PQ became a challenge to the power engineers. The regulation of capacitor voltage across the DC-Link in addition to minimization of THD in current waveforms, improving PF, and elimination of voltage sag, swell, disturbance, flicker and voltage unbalances to improve the stability and reliability of the grid. To improve the PQ, FACTS device used at the Distribution side of the utility grid is the UPQC.

B. LITERATURE REVIEW

The THD is a significant measure of PQ and it is must to keep it as low as possible. Lower the THD higher the efficiency, PF, and life duration of equipment [1]. The advancement in power electronics has contributed to active power filters involving VSCs for mitigating PQ issues. The UPQC, an important member of the FACTS family employing two back-to-back VSCs, finds more applications in addressing the PQ issues than those of other FACTS devices [2]. The PV associated UPQC was developed with a view to minimize the THD, voltage distortions, and compensating reactive power by extracting the maximum power from the PV panel by adopting MPPT technique [3]. Meanwhile, different artificial-Intelligent Control techniques like FL-C and ANN for improving PQ in the grid connected distribution network were outlined [4]. The development of intelligent algorithms enables the online control of APF in UPQCs through PI-C, FL-C, SM-C, and ANN [4], [5], [6] for improving PQ for varying nonlinear loads.

Recently, an artificial-neuro fuzzy interface system-based controller was designed for solar integrated UPQC for PQ improvement. The performance analysis was done for various combinations of loads and supply conditions to exhibit the superiority of the proposed technique [7].In addition; an UPQC associated with a PV system with PI-C was designed with the goal of minimizing the distortions associated with voltages and currents. The PV system was coupled to the DC-link through a BC. The compensation to voltage interruptions and power transfer under islanding were also discussed [8].

The FL-C based controller was developed for the multi-converter UPQC to address the PQ issues effectively [9]. The predator-prey firefly optimization technique was applied in optimally designing shunt active power filters with the objective of minimizing THD and improving power factors [10]. Solar, wind, and fuel cell integrated multi-level UPQC was designed with a view of diminishing the voltage distortions like sag, swell, disturbances, and harmonics in the source currents by injecting suitable voltage and currents [11]. The Predictive phase dispersion modulation technique was implemented on Cascaded H-Bridge Multi-Level UPQC with the motive of compensating the voltage fluctuations, harmonics in current waveform, and maintaining stable DC-Link voltage [12]. Various PQ issues, different design schemes, and THD reduction methods for UPQC were reviewed in detail [13]. THD minimization of induction-furnace load at the steel plant with an UPQC was carried out and to exhibit its superiority the comparative analysis was done with a synchronous compensating device [14]. The development of ANN-based controller for UPQC and its performances were studied by considering issues like sag, swell, harmonics supply voltage, and unbalanced nonlinear loads. The significance of DC-link capacitor voltage on supply currents and THD's was also discussed [15].

A nonlinear SM-C along with real and reactive power hypothesis was developed for UPQC with a view of effectively compensating voltage and current distortions. The controller provided a complete and fast response for compensating the voltage sags/swells and unbalanced supply voltages [16]. The UPQC employed with solar PV-wind-fuel cell-battery system is proposed to minimize the various power quality issues [17]. An Ant colony algorithm based optimal tuning of PI- was designed for SHAPF to minimize THD for different combinations of loads [18].

A hybrid fuzzy back-propagation control scheme based on 5-level UPQC was proposed to minimize the THD and improve the PF [19]. The SOL based load flow (LF) for both transmission and distribution systems was presented with a objective of minimizing the sum of the squares of the active, and reactive power mismatches at all the busses, while considering the net deviations of bus voltage angles, and magnitudes as unknown variables [20]. An Adaptive full order observer based control algorithm was developed for the UPQC to improve the PQ due to its fast response in fault detection for all positive sequence components, and high accuracy in monitoring under all various loads / grid conditions. In addition, a BBO algorithm was employed for the optimal tuning of Kp and Ki values for PI-C on UPQC with a view of minimizing the DC-Link voltage oscillations [21]. However, the PQ issues for the micro-grid integrated distribution network were addressed using UPQC in order to mitigate voltage imbalances and current harmonics. Adaptive network-based fuzzy inference system was proposed to maximize the utilization and the efficiency of the system [22].

An automated shifting method between the grid and island modes was developed for PV battery integrated UPQC in the view of addressing the PQ issues with low disturbance to the local loads. Further, the system performance was validated with experimental results [23]. Beside, the grid connected network with an adaptive FL-C based on series active power filter was designed to address the PQ problems like voltage fluctuations/interruptions, reduction of current harmonics, and maintain of constant DC-Link voltage [24]. The combination of both Improved Bat Algorithm and Moth Flame Algorithm optimization based hybrid control technique was developed to address the PQ issues in micro-grid system with a view of minimizing the error function of power variation. In addition, operation cost of renewable sources was also reduced with optimal tuning of Kp and Ki parameters [25].

An ANN controller based on the hybrid combination of reactive power control with unit vector template generation was designed for UPQC with an objective to mitigate PQ issues effectively. In addition, solar PV connected in order to reduced the ratings of then power converters, and stable the DC-Link capacitor voltage during faulty and load variation conditions [26]. Besides, the novel sequence-component detection method hybridized with unit vector-template generation was proposed for the double stage solar integrated UPQC with a goal of diminishing PQ issues [27]. The review of various topologies, compensation techniques, controllers, and the technological advancements of the recent years for the UPQC were outlined with a motive of eliminating of PQ issues [28].

A SMC based adaptive linear neuron-proportional resonant control method was developed to enhance performance of Vienna rectifier, an AC–DC converter, as a charger for series-linked battery packs of electric vehicles operating under unbalanced and distorted grid conditions. In addition, reference current signals are generated without sequences component separation, coordinate transformation and phase-locked loop to achieve superior dynamic and steady-state performances and eliminate harmonics of source currents and ripples in active power, DC-link voltage and battery current compared to the existing studies [29]. The proposes a coordinated virtual impedance control scheme for a vehicle to grid three phase four leg (V2G 3p4L) inverter was proposed with an objective of objectives consisting of

effective and good harmonic rejection capability, power sharing among V2G 3p4L inverter units with a smaller error, reactive power/voltage support during load power changes and balanced/unbalanced voltage sag conditions. In addition, technique exhibits superior performance for both grid and island modes [30].

A Lyapunov proportional integral with anti-windup (PI with AW) control is proposed to regulate oscillations of the DC-link voltage without increasing DC-link capacitor size, harmonic compensation and charging through three-phase SHAPF as interface EV applications and the electric grid was designed for effective harmonics mitigation under various non-linear loads (NLLs) groups and grid disturbances [31]. A swarm intelligence tuned Kalman filter based PV integrated SHAPF was designed with an objectives of maintaining sinusoidal waveform at the common utility point, unity PF, reduction of harmonics and improvement of overall performance. To show the superior performance of proposed method different case studies with balanced/ unbalanced loads and supply voltages with variable irradiations was analyzed [32]. Adaptive generalized maximum Versoria criterion (AGMVC) controller was suggested for PV associated VSC to address PQ issues such as harmonics, redundant reactive power and load unbalancing. To exhibit viability of proposed technique is compared with synchronous reference frame theory (SRFT) and instantaneous reactive power theory (IRPT), least mean square (LMS), least mean mixed norm (LMMN) and normalized kernel least mean fourth-neural network (NKLMF-NN). In addition, performance of AGMVC control technique is verified experimentally using laboratory prototype with dSPACE DS-1202 [33].

An Euclidean direction search (EDS) technique based adaptive control theory was designed for three-phase four-wire distribution static compensator (DSTATCOM) for elimination of several power quality (PQ) issues, namely harmonics, reactive power, load unbalancing, and neutral current. The real-time performance investigation was carried out of using dSPACE1104 R&D controller [34]. Although quite a lot of techniques were recommended in the literature review, still there is a possibility for designing new controllers and techniques for efficiently eliminating the PQ problems.

C. KEY CONTRIBUTION

This study is to enhance the PQ in Distribution network. The highlights of this article are emphasized below:

- Design of Hybrid controller involving fuzzy logic and soccer league algorithm optimal tuned PI-C (SLOHC) for Solar PV and BS integrated UPQC (U-PVBS).
- The prime aim of the proposed method is to minimize THD thereby improving PF, eliminate sag/swell/large disturbance in source voltage and maintain constant DC-Link voltage.
- The results are obtained for variation in loads, PV-irradiation, and supply voltage as case studies.
- Future, performance analysis was carried out with standard methods like a GA, BBO, and PI-C. To exhibit the superiority of the proposed technique comparison was done with those of existing methods available in literature review.

However, from the literature survey as shown in Table 1, it is clearly noticed that the majority of research papers focused mainly on THD reduction and or DC-Link voltage regulation with sag/swell elimination as their main objectives with the various controllers. In the proposed work along with the optimal tuning of PI controller K_p and K_i values for the THD minimization, the DC-Link voltage balancing for solar irradiation variation, the PF improvement was also considered. However, along with sag/swell the voltage disturbance is also considered as PQ issues for different combination of balanced/ unbalanced non-linear loads and supply voltage with fuzzy based SLOHC for optimal instead of conventional methods.

D. PAPER ORGANIZATION

The proposed paper involves the design of SLOHC for solar battery integrated UPQC to enhance PQ. Section 2 deals with the configuration, components and working of U-PVBS along with the Shunt and series converter controllers, section 3 discusses proposed soccer league optimization, section 4 deals with fuzzy controller and lastly, section 5 gives the conclusion.

II. PROPOSED U-PVBS

Figure1 gives the layout of UPQC with the external support of BS with BBC and solar PV system with BC connected to DC-link. This paper proposes SLOHC for exploiting both the properties of the FL-C and optimally tuned PI-C. V_a, V_b, V_c are the grid voltages, $V_{S\_a}, V_{S\_b}, V_{S\_c}$ are source phase voltages, R_s, L_S are source side resistance and inductances. UPQC is made of the series and shunt converters connected via a DC-Link. The SAPF eliminates the supply voltage related distortions and unbalances by injecting the suitable compensating voltage V_{se} through an isolating transforms. It consists of series-resistor R_{se}, series-inductor L_{se} and series-capacitor C_{se}.

The SHAPF consist of a shunt-resistance R_{sh}, shunt-interfacing inductor L_{sh}, shunt-capacitance C_{sh}. It reduces the harmonics in current waveform and regulates the DC-link capacitor voltage (V_{dc}) stable during load and irradiation variations by injecting a suitable compensating shunt current i_{sh}. The U-PVBS specifications, ratings of the loads considered were exhibited in Table 2.

A. EXTERNAL SUPPORT OF DC-LINK

The SP and BS acts as external support to the DC-Link via a BC and BBC with a view of maintaining stable DC-Link voltage during load/solar irradiation variations, minimizing PQ issues as figure 2. The power balance equation of U-PVBS at

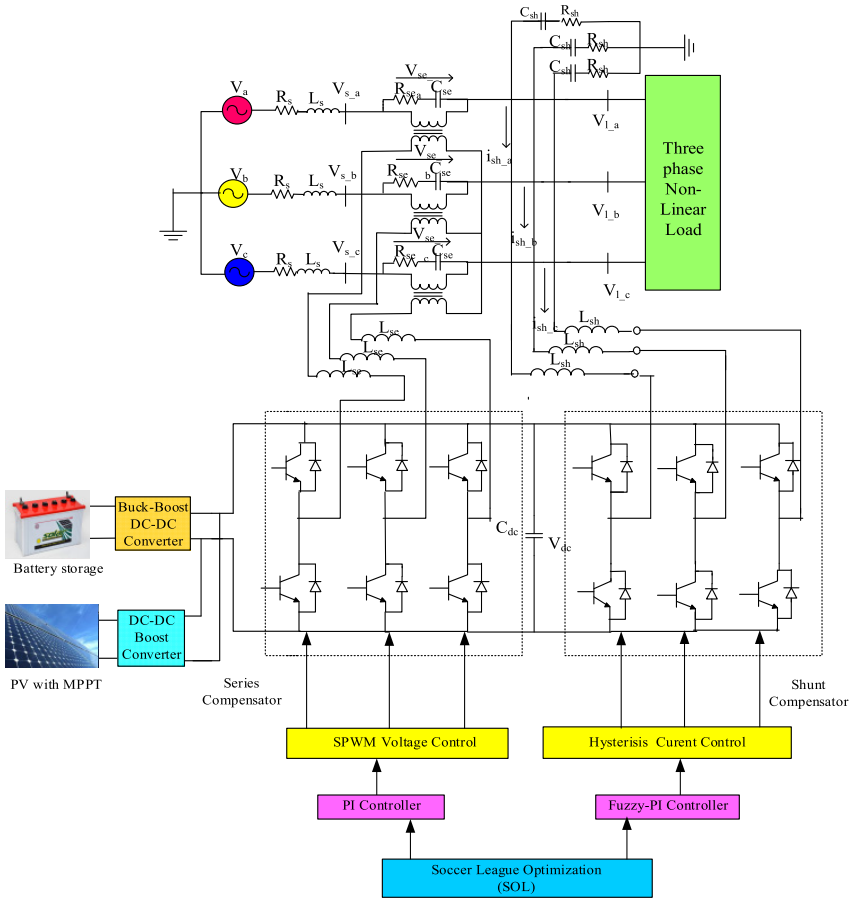

FIGURE 1. Structure of solar PV and BS integrated UPQC.

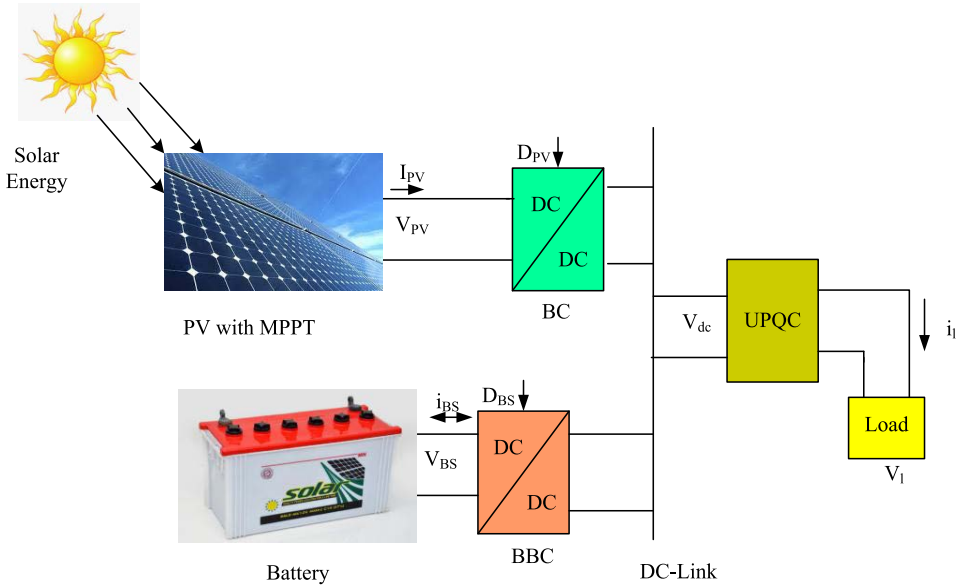

FIGURE 2. External support of DC-Link.

the DC-Link is as given in Eq. (1).

$$P_{PV} + P_{BS} - P_{dclink} = 0 \tag{1}$$

where, P_{PV} and P_{BS} denote the output power of solar and battery systems.

P_{dclink} denotes the power demand at DC-Link.

TABLE 1. literature review.

Controller [Ref]	PQ issues / Loads considered									
	THD	PF	DC-Link balancing	Voltage sag/swell	Voltage disturbance	Supply voltage Imbalance	Non-linear load	Un-balanced non-liner load	Induction Furnace load	Induction Motor Load
ANFIS [7]	✓			✓			✓			
PI-C [8]	✓		✓		✓					
FL-C [9]	✓			✓			✓			
PPFO [10]	✓	✓				✓	✓	✓		
FL-C [11]				✓	✓		✓			
Predictive Phase Dispersion[12]	✓		✓		✓		✓			
PI-C [14]	✓								✓	
ANN [15]	✓		✓	✓				✓		
SM-C [16]	✓			✓		✓	✓			
BF-PI-C	✓			✓			✓			
ANN [18]	✓						✓	✓		✓
Fuzzy Back propagation [19]	✓			✓				✓		
BBO [21]	✓		✓	✓			✓	✓		
ANFIS [22]	✓					✓				
FL-C [24]	✓		✓	✓			✓			
Improved Bat & Moth Hybrid Algorithm[25]	✓						✓			
ANN [26]	✓						✓			
SLOHC	✓	✓	✓	✓	✓	✓	✓	✓	✓	✓

TABLE 2. UPQC specifications and Loads.

Source side	Voltage =415V ; Frequency =50Hz Resistance =0.1 Ω ; Inductance = 0.15 mH
Series-compensator	Resistance =1.0Ω ; Inductor=3.60mH ; Capacitor= 60.0 µf
Shunt-compensator	Resistor= 0.0010Ω ; Inductor= 2.150mH ; Capacitor= 1.0 µf , Hysteresis band: 0.010A
Dc-Link	DC-Link capacitor= 9400 µf ; Voltage at DC-Link =700 V
Loads	1. Balanced 3 Φ Rectifier load: R=10.0Ω, L=40.0mH. 2. Unbalanced 3 Φ R-L load: R1=10.0Ω, L1=9.50mH, R2=20.0 Ω, L2=10.50mH, R3=15.0 Ω, L3=18.50 mH. 3. Induction Motor Load: LC = 400 mH, 50 µF, RL = 10Ω, 100 mH. 4. Induction Furnace load: LC = 400.0 mH,50.0 µF, RL = 10.0 Ω,100.0 mH

TABLE 3. BS and solar-PV specifications.

Device	Parameters	Values
Li-ion battery	Rated-capacity	350 Ah
	Max-capacity	450 Ah
	Nominal-voltage	650 V
	Full charge-voltage	756 V
	Open-circuit voltage	48.3 V
	Short-circuit current	5.8 A
Solar-PV panel (SPR-215-WHT-U)	Voltage/current at max power	39.80 V /5.40A
	Total parallel cells	11
	Total series cells	18

B. SOLAR PV SYSTEM

Solar energy is the non-conventional energy source, preferred it is freely available, clean, and pollution free. The UPQC can be connected with distributed energy resources like solar, wind, fuel cell, etc. In this paper PV is connected at the DC-link element for the following reasons outlined below:

- It enhances PQ at the utility grid
- It reduces the supply side demand
- It protects the loads from grid disturbances
- It reduces the stress and voltage ratings of the converter

In general, the PV panels are arranged in a series and or parallel connection to produce the required DC power. Further, it can be boosted up to the desired level with the help of BC. However, the SP charges the capacitor of DC-Link in addition to the real power exchange during load variations. Hence, MPPT controller is necessary to extract the maximum power from the PV panels. The controller of the SP with MPPT, a BC to boost up the output voltage cell was exhibited in figure 3 while figure 4 provides the basic working model of PV cell. The output power P_{PV} of the SP can be calculated by using the Eq. (2).

$$P_{PV} = V_{PV}.I_{PV} \tag{2}$$

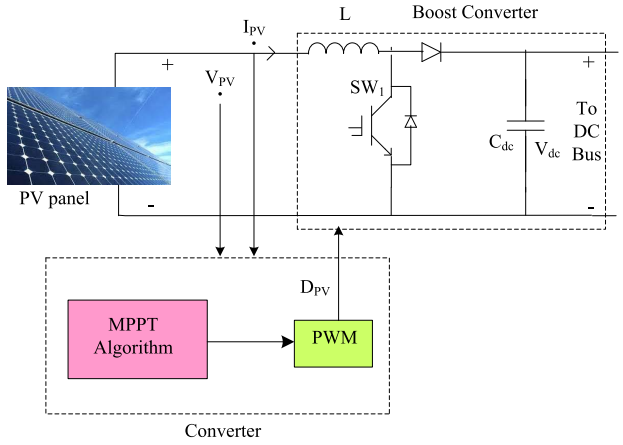

FIGURE 3. Solar PV with controller.

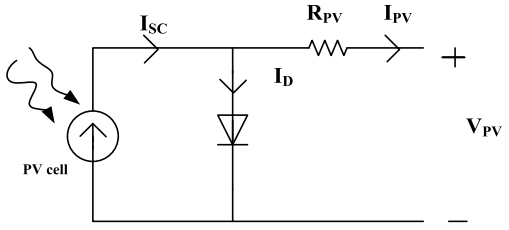

FIGURE 4. Model of PV solar cell.

In this work, one of the most familiar MPPT technique i.e., P&O algorithm was adopted. The ratings of SP, BS are given in Table 3.

C. BATTERY-STORAGE SYSTEM

The BS consists of a battery, BBC with PI-C, for regulating the stable DC-Link voltage as figure 5. The *SOC* plays a vital role in improving the performance and overall life of the battery given by Eq. (3).

$$SOC = 100(1 + \int i_{BS}\ dtQ) \tag{3}$$

In general, it works on two modes; charging or discharging which mainly depends on the amount of solar power generated. The *SOC* limits are given by Eq. (4).

$$SOC_{\min} \leq SOC \leq SOC_{\max} \tag{4}$$

The reference current i_{dc}^{ref} is approximated by reducing the of DC-Link voltage error $V_{dc,error}$ using a PI-C controller in mathematic terms, the approximation can be explained as given in Eq. (5) and (6).The battery error current reference $i_{BS,error}^{*}$ is obtained by PI-C of battery error current.

where, $i_{BS,error}$ is the difference between the reference DC-Link current i_{dc}^{ref} and reference battery current i_{BS}^{ref} given in Eq. (7) obtained from LPF is given in Eq. (8), (9).

$$V_{dc,error}(t) = V_{dc}^{ref} - V_{dc} \tag{5}$$

TABLE 4. Power sharing at DC-link.

Level of SPG	Power Distribution
SPG > P_{dclink}	BS charges until it reaches to $SOC_{\max}$
SPG = P_{dclink}	SP only supplies P_{dclink}
SPG < P_{dclink}	BS supplies the difference amount of power till it reaches the lowest limit of $SOC_{\min}$
No SPG	BS supplies P_{dclink}

$$i_{dc}^{ref} = K_{p1}\ V_{dc,error}(t) + K_{i1} \int_0^t V_{dc,error}(t)\ dt \tag{6}$$

$$i_{BS,error}(t) = i_{dc}^{ref} - i_{BS}^{ref} \tag{7}$$

$$i_{BS,error}^{*} = K_{p2}\ i_{BS,error}(t) + K_{i2} \int_0^t i_{BS,error}(t)\ dt \tag{8}$$

where,

$$i_{BS}^{ref} = \left(\frac{1}{1 + T.S}\right) * i_{BS} \tag{9}$$

PI-C_1, PI-C_2 gains are heuristically chosen as $K_{p1} = 1.5$, $K_{i1} = 0.1$, $K_{p2} = 1.477$ and $K_{i2} = 3.077$. Table 4 gives the power sharing between SPG, BS and DC-Link power demand under different operating conditions of the U-PVBS.

D. SHUNT CONVERTER

The shunt converter performs the dual function of compensating harmonics in load current waveforms thereby improving PF, and supplying solar power to maintain constant and stable DC-Link voltage during load variations. The shunt-VSC adapts (i) abc-dq0 and dq0-abc domain conversions, (ii) firefly based PI-C with FL-C. The load current is converted into dq0 domain by using the phase/ frequency information of the grid voltage using PLL. Both the FL-C and firefly based PI-C compares the DC-link voltage with the reference voltage and converts the error voltage into a required change in current for regulating the DC-link capacitor voltage. The q-th component load current is added with the error current signal derived from FL-C and optimal designed PI-C. The dq0 components are again transformed into abc domain, which are compared with the actual load currents in a hysteresis current-controller to produce appropriate gate pulses for shunt VSC as in figure 6.

E. SERIES CONVERTER

During under/over loading conditions at the load side, the grid supply voltage may fluctuate. The control signals are produced by comparing the actual load voltage with the reference voltage through a optimally designed PI-C after transformations from abc-to-dq0 domain. Later, it is again transformed into abc domain as in figure 7. The control signals serve

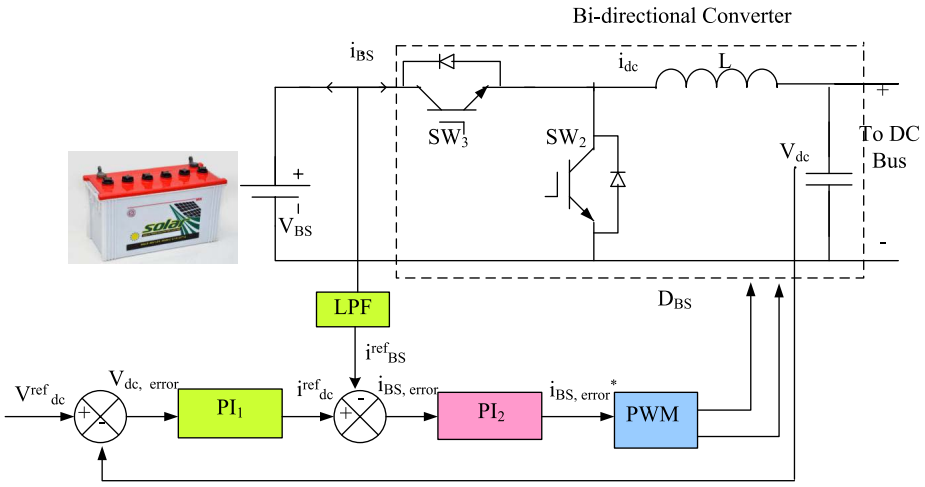

FIGURE 5. Battery storage with Bi-Directional Buck Boost converter.

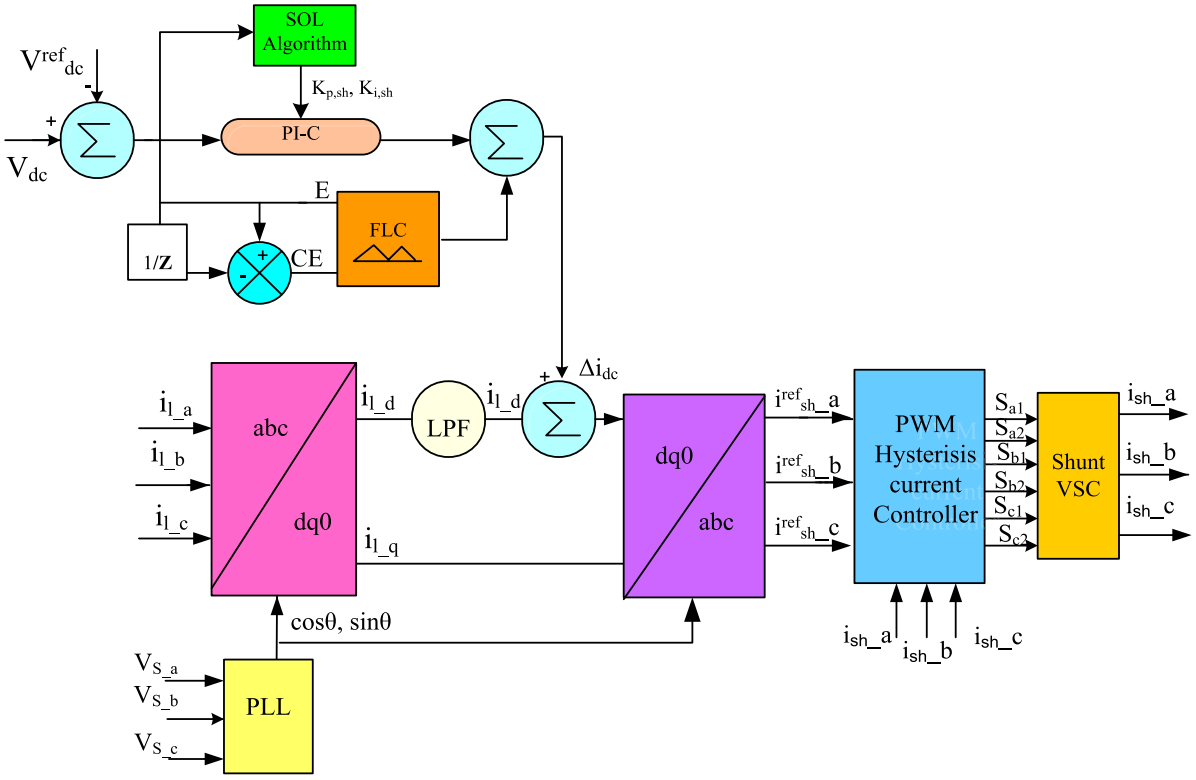

FIGURE 6. Soccer league optimization based hybrid controller for Shunt Converter.

as gating pulses for performing PWM in a series converter. As abc to dq0 and dq0 to abc domain transformations are available in the literature, the design of firefly optimization-based PI-C and fuzzy control part is explained below chapter.

III. SOCCER LEAGUE OPTIMIZATION

SOL is a population-based sports algorithm that is derived from the competition behaviour of players within the team and with the other teams of the league [20]. The performance of each player can be improved by competing with another player, thus by improving the strength of the team. This paper provides soccer league optimization with a view of improving

TABLE 5. Chosen parameters.

Algorithm	Parameter	Chosen Value
SOL	nap	6
	nsp	4
	m	4

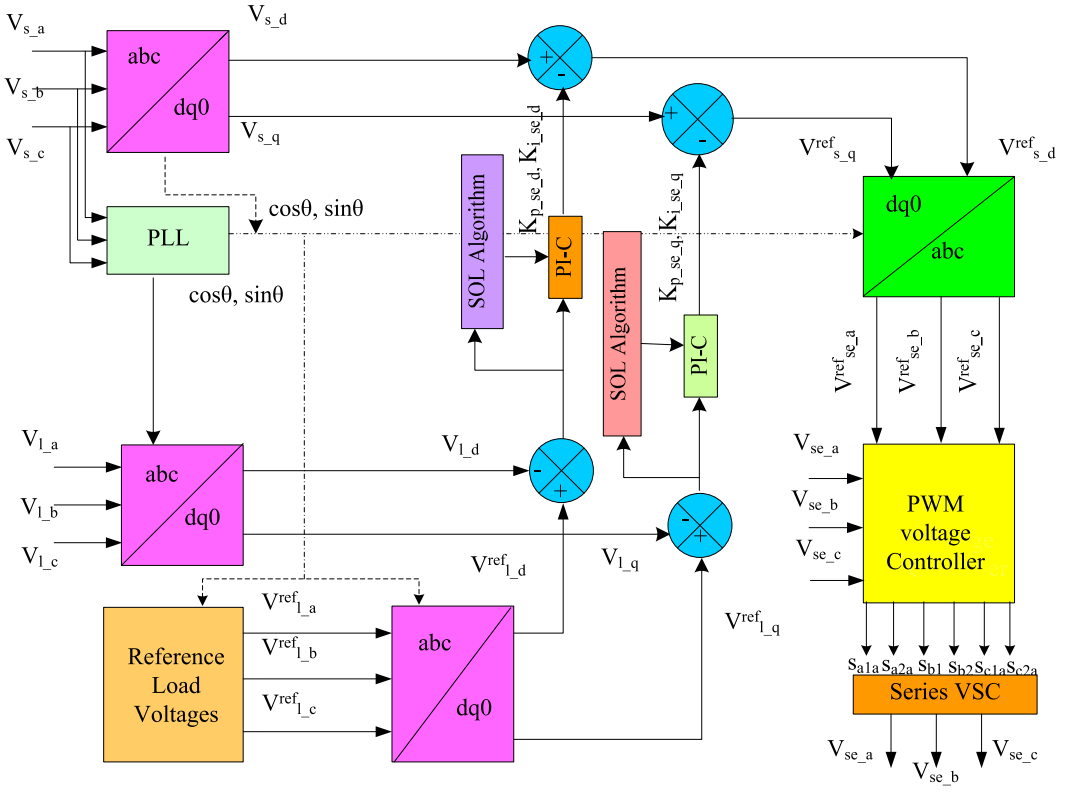

FIGURE 7. Soccer league optimization based hybrid controller for Series Converter.

the THD thereby PF and elimination of voltage distortions by optimally designing the PI-C.

The proposed algorithm chooses the K_p, K_i of the PI-C for shunt and series converters as problem variables, and the formation of the fitness function. The tuning of PI-C can be treated as an optimization problem with a view of minimizing the THD through optimally choosing K_{p_sh}, K_{i_sh}, $K_{p\_se\_d}$, $K_{i\_se\_d}$, $K_{p\_se\_q}$, $K_{i\_se\_q}$ parameters. In this approach, each player (y) is treated as a selected design parameter represented in vector form given in Eq. (10). While the upper and lower bonds are given in Eq. (11).

$$y = [K_{p\_sh}, K_{i\_sh}, K_{p\_se\_d}, K_{i\_se\_d}, K_{p\_se\_q}, K_{i\_se\_q}] \quad (10)$$

The constraints are represented as

$$y^k(\min) \le y^k \le y^k(\max); \quad k = 1, 2 \ldots nd \quad (11)$$

where, nd = number of design variables

The total number of players are randomly produced and clustered into the number of teams. Each and every team consists of a set of active-players (APL's), and substitute-players (SPL's). In any team each player has his/her own skills which are represented in Eq. (12).

$$[y^1_{kj},\ y^2_{kj},\ \cdots,\ y^{nd}_{kj}] = [K_{p\_sh}, K_{i\_sh}, K_{p\_se\_d}, K_{i\_se\_d}, K_{p\_se\_q}, K_{i\_se\_q},] \quad (12)$$

The total number of players (population) and their teams (T) are denoted as in Eq. (13)

$$\textit{Population} = \begin{bmatrix} T_1 \rightarrow AT_1 = \begin{Bmatrix} APL_{1,1} \\ APL_{1,2} \\ \vdots \\ APL_{1,nap} \end{Bmatrix}; ST_1 = \begin{Bmatrix} SPL_{1,1} \\ SPL_{1,2} \\ \vdots \\ SPL_{1,nsp} \end{Bmatrix} \\ T_2 \rightarrow AT_2 = \begin{Bmatrix} APL_{2,1} \\ APL_{2,2} \\ \vdots \\ APL_{2,nap} \end{Bmatrix} ST_2 = \begin{Bmatrix} SPL_{2,1} \\ SPL_{2,2} \\ \vdots \\ SPL_{2,nsp} \end{Bmatrix} \\ \vdots \qquad\qquad \vdots \\ T_m \rightarrow AT_m = \begin{Bmatrix} APL_{m,1} \\ APL_{m,2} \\ \vdots \\ APL_{m,nap} \end{Bmatrix} ST_m = \begin{Bmatrix} SPL_{m,1} \\ SPL_{m,2} \\ \vdots \\ SPL_{m,nsp} \end{Bmatrix} \end{bmatrix} \quad (13)$$

where,

$APL_{k,j}$ is the jth APL of kth team.

$SPL_{k,j}$ is the jth SPL of kth team.

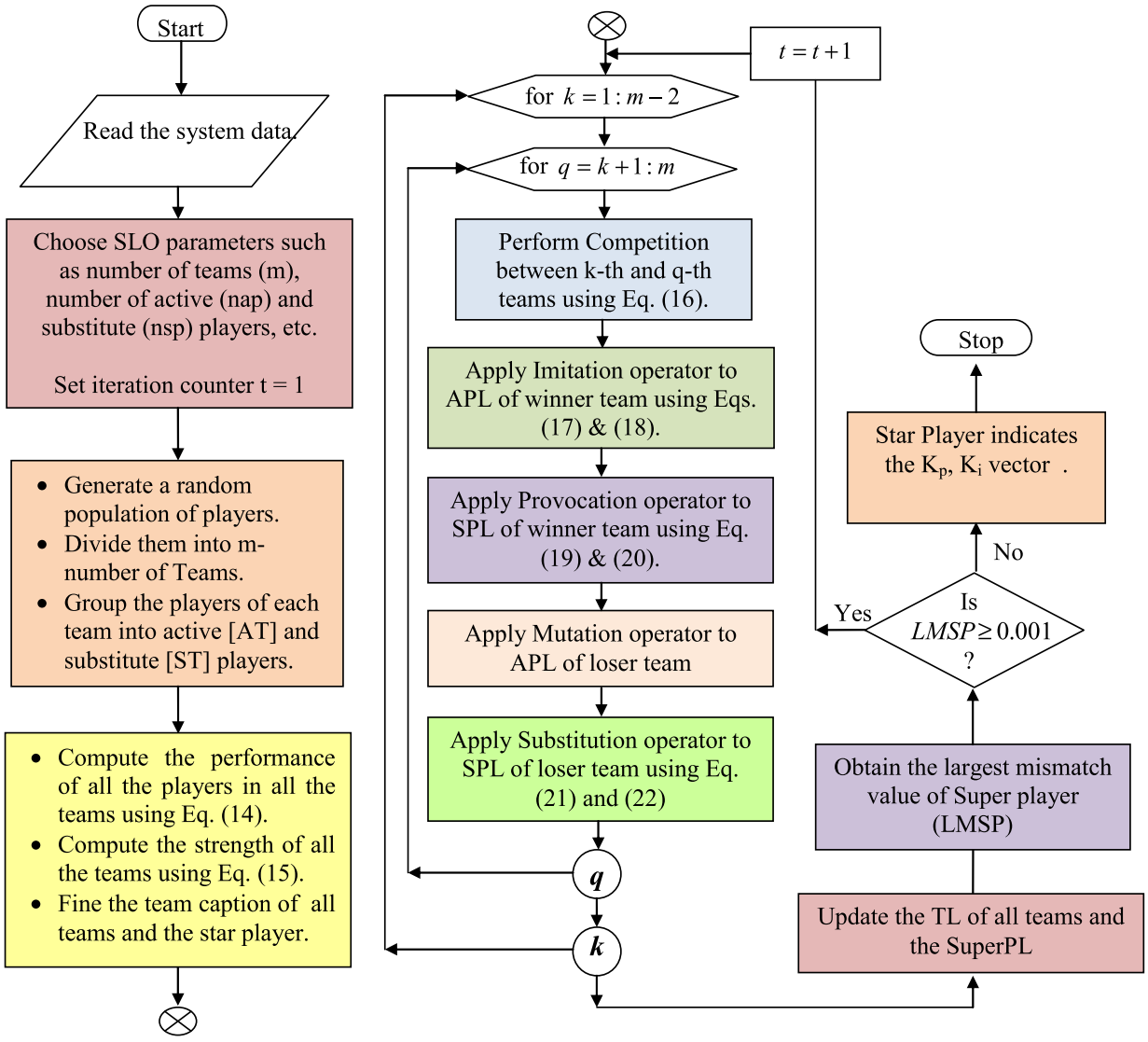

FIGURE 8. Flowchart of soccer league optimization based UPQC.

nap and *nsp* denotes the number of APL's and SPL's respectively.

AT_k is the kth active-team with nap.

ST_k is the kth substitute-team with nsp.

nd denotes the total number of control variables.

m denotes the number of teams.

In a team the fitness of each player depends on his/her skills and it is calculated by a performance function (FF_{kj}), derived from the objective function (THD of source current). The max performance function indicates the lower objective function as given in Eq. (14).

$$MaxFF_{kj} = \frac{1}{1 + THD} \tag{14}$$

A probability of the team to win the league depends on the strength of the payers. The strength of kth team (ST_k) can be calculated by Eq. (15).

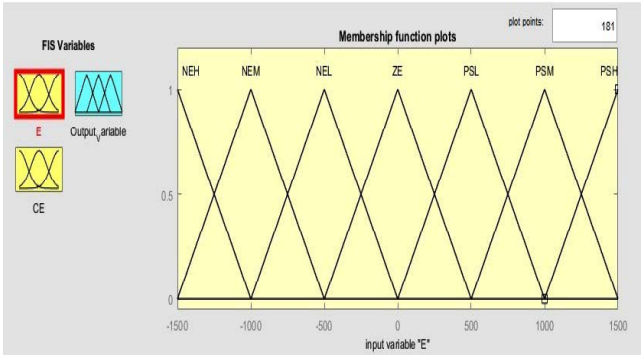

FIGURE 9. Member ship function for "error" of shunt controller.

$$ST_k = \sum_{j=1}^{nap+nsp} \frac{FF_{kj}}{nap + nsp} \tag{15}$$

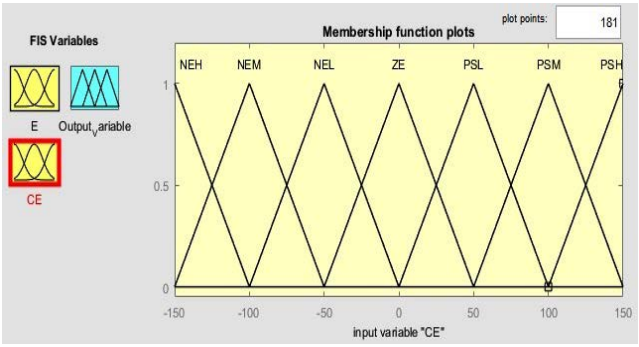

FIGURE 10. Member ship function for "change in error" of shunt controller.

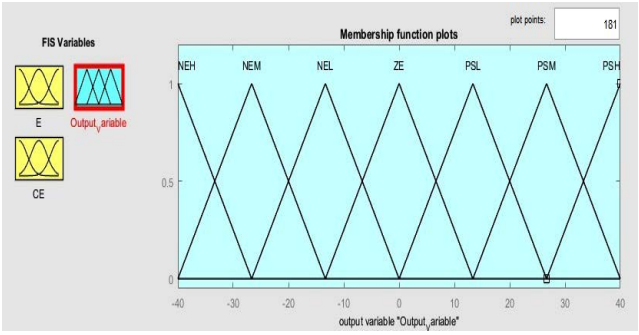

FIGURE 11. Member ship function for "output (duty cycle)" of shunt controller.

TABLE 6. Fuzzy if-then rules.

E	COE						
	PSH	PSM	PSL	ZE	NEL	NEM	NEH
NEH	ZE	NEL	NEM	NEB	NEH	NEH	NEH
NEM	PSL	ZE	NEL	NEM	NEH	NEH	NEH
NEL	PSM	PSL	ZE	NES	NEM	NEH	NEH
ZE	PSH	PSM	PSL	ZE	NEL	NM	NEH
PSL	PSH	PSH	PSM	PSL	ZE	NEL	NEM
PSM	PSH	PSH	PSH	PSM	PSL	ZE	NEL
PSH	PSH	PSH	PSH	PSH	PSM	PSL	ZE

The player having the largest fitness value in each (k^{th}) team is considered as team leader (TL_k), and the best player among all team leaders, is called the super player (SuperPL) of the league. The probability of winning of k^{th} over q^{th} team is given by Eq. (16).

$$\left\{\begin{array}{l}\text{if } rand() < \left(\frac{ST_k}{ST_k+ST_q}\right), \\ \text{k-th team is winner \& q-th team is loser} \\ \text{else} \\ \text{k-th team is loser \& q-th team is winner} \\ \text{end}\end{array}\right\} \quad (16)$$

Once the match is completed, the players of winning team and losing team implement certain actions for their performance enhancement. The mathematical representation of these actions in a form of operators is given below:

Imitation Operator: The APL's of the champion team tries to imitate the TL and SuperPL for the performance enhancement given by Eq. (17) and (18).

$$APL_{kj} = \mu_1 APL_{kj} + \tau_1(SuperPL - APL_{kj}) + \tau_2(TL_k - APL_{kj}) \quad (17)$$

$$APL_{kj} = \mu_2 APL_{kj} + \tau_1(SuperPL - APL_{kj}) + \tau_2(TL_k - APL_{kj}) \quad (18)$$

where, μ_2, μ_1, τ_1 and τ_2 are random numbers.

If the performance of APL's is better than old one, then $APL_{k,j}$ carry out large movements by Eq. (17). Or else, the player shifts towards the medium movements by Eq. (18). If there is no improvement from the above actions, the player will be retained in previous position.

Provocation operator: The SPL's tries to perform better than those of APL's of the winner team. The SPLs move towards the average direction of APL's using Eq. (19) and (20).

$$SPL_{kj} = D(k) + \chi_1(D(k) - SPL_{kj}) \quad (19)$$

$$SPL_{kj} = D(k) + \chi_2(SPL_{kj} - D(k)) \quad (20)$$

where, χ_1, and χ_2 are random numbers, $D(k)$ is the mean direction of APL's in winner's team. SP_{kj} is the j-th substitute of k-th team.

If the performance of APL's is better than the old one then the SPL_{kj} performs forward move in the average direction of APL's by using Eq. (19). Or else, the player takes back movement by Eq. (20). If there is no performance improvement from the above movements, he/she is replaced by a vector with a random solution.

Mutation operator: The APL's of the loser team try to explore possible ways for enhancing their performance during this process they randomly change their positions by adopting the mutation operator.

Substitution Operator: To escape from the local traps the loser's team creates a fresh combination of substitutes (j and p) by integrating two of the existing members by Eqs. (21) and (22).

$$SPL_{kj} = \alpha\ SPL_{kj} + (1-\alpha)\ SPL_{kp} \quad (21)$$

$$SPL_{kp} = \alpha\ SPL_{kp} + (1-\alpha)\ SPL_{kj} \quad (22)$$

where, α is a random number.

The main aim of using SOL in this work is its superior performance in solving multi-objective optimization problems with faster convergence, accuracy and cost effective. Compare to conventional algorithms like GA, PSO it has the lowest sensitivity to the problem's dimensions [23]. It can also be implemented on both linear and non-linear loads. However, it has its own limitation like complexity as the number of control variables increases. In order to satisfy the equality constraints, single objective function was selected

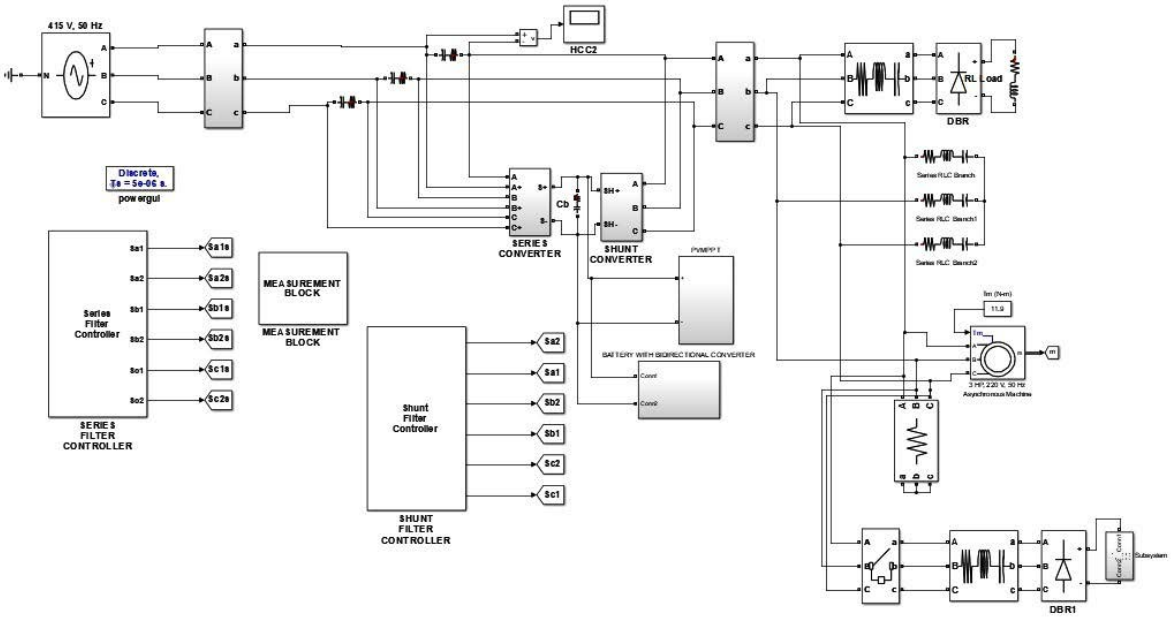

FIGURE 12. Simulink model of solar PV battery integrated UPQC along with loads.

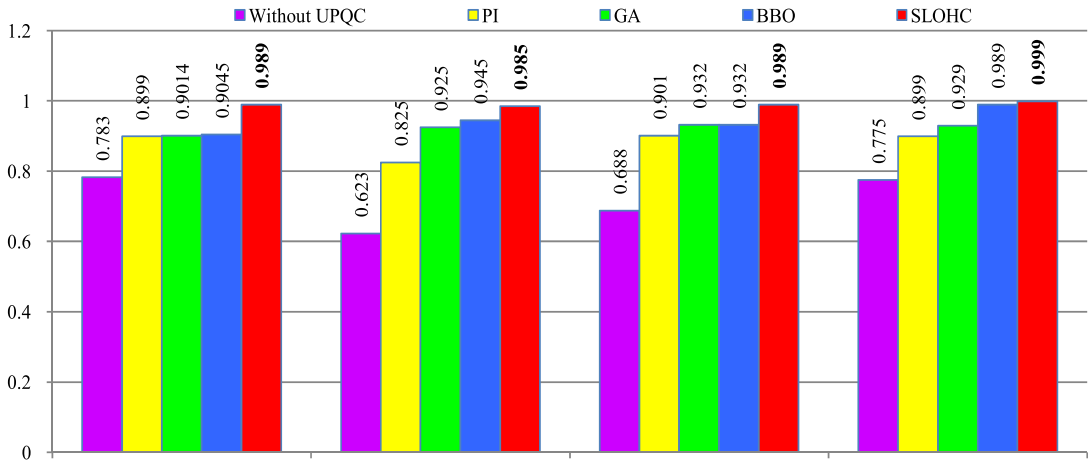

FIGURE 13. Comparison of power factors.

TABLE 7. Test cases considered.

Condition	Case1	Case2	Case3	Case4
Balanced source voltage	✓	✓	✓	
Unbalanced source voltage				✓
Steady state voltage				✓
Voltage Sag	✓			
Voltage Swell		✓		
Voltage disturbance			✓	
Solar Irradiance at1000	✓	✓		✓
Solar Irradiance at 800			✓	
Balanced Rectifier Load	✓	✓		
Unbalanced RL Load			✓	✓
Induction Motor Load		✓		✓
Induction Furnace load			✓	

and the decision vector structure designed such a way that only the valid manifold is searched so that every random solution automatically has the constraint satisfied.

However, the drawback of conventional PI controller is poor selection of K_p, K_i values but by adopting SOL based tuning method the algorithm automatically

TABLE 8. %THD comparision.

Method	Case1	Case2	Case3	Case4
Without U-PVBS	27.67	15.89	33.91	7.33
PI-C	6.20	7.37	7.51	4.02
GA	4.41	5.12	5.40	2.58
BBO	4.05	4.59	3.02	2.96
PI-C [16]	3.28	--	--	--
SM-C [16]	2.44	--	--	--
BBO [21]	4.13	--	--	--
PI-C [22]	14.74	--	--	--
FL-C [22]	6.13	--	--	--
ANFIS [22]	2.43	--	--	--
PI-C [24]	3.65	--	--	--
FL-C [24]	2.52	--	--	--
Conv. PI-C [17]	3.88	--	--	--
ACO-PI-C [17]	3.72	--	--	--
BF-PI-C [17]	3.71	--	--	--
PSO [10]	2.109	--	--	--
HSO 10]	2.231	--	--	--
ZN [10]	7.57	--	--	--
ICM [10]	4.2	--	--	--
SLOHC	**2.06**	**2.44**	**2.40**	**2.32**

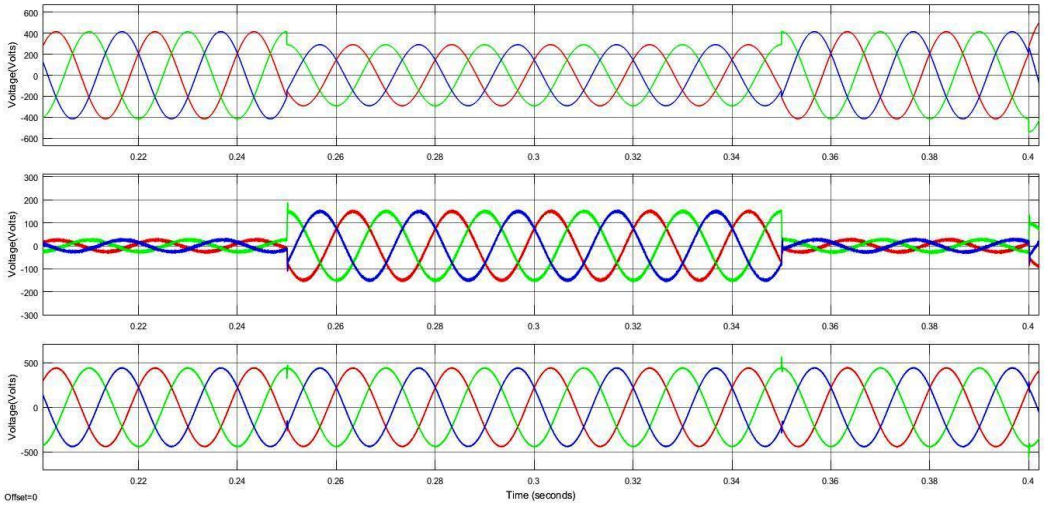

(a) Source voltage, Injected voltage, Load voltage

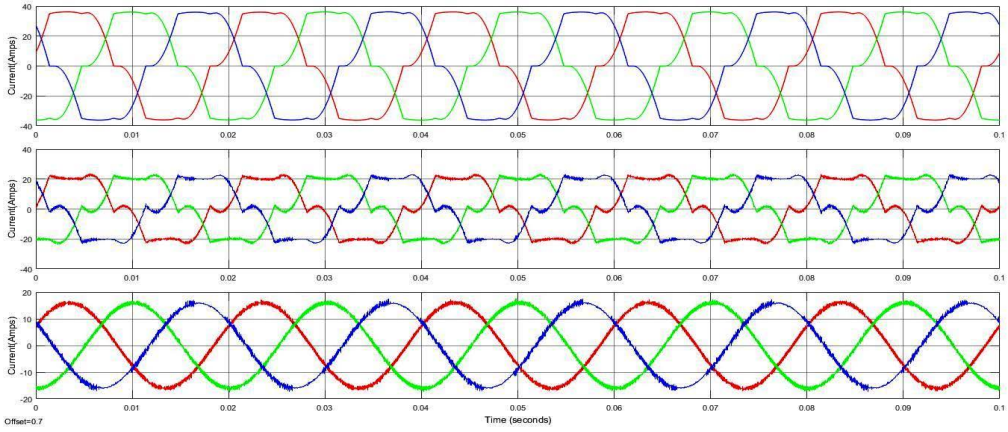

(b) Load current, Injected current, Source current

FIGURE 14. Waveforms of the proposed system for case-1.

tune K_p, K_i according to the required objective function within the given range with less execution time and high accuracy.

The flowchart as in figure 8 gives the design method of the proposed SOL for optimal selection of K_p, K_i values for series and shunt converters. The star players of the match indicates

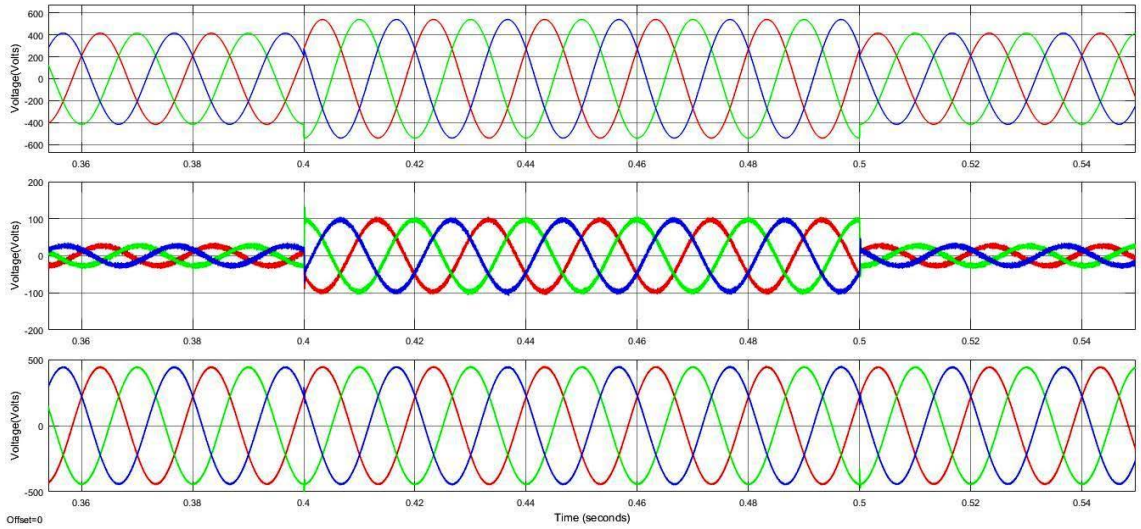

(a) Source voltage, Injected voltage, Load voltage

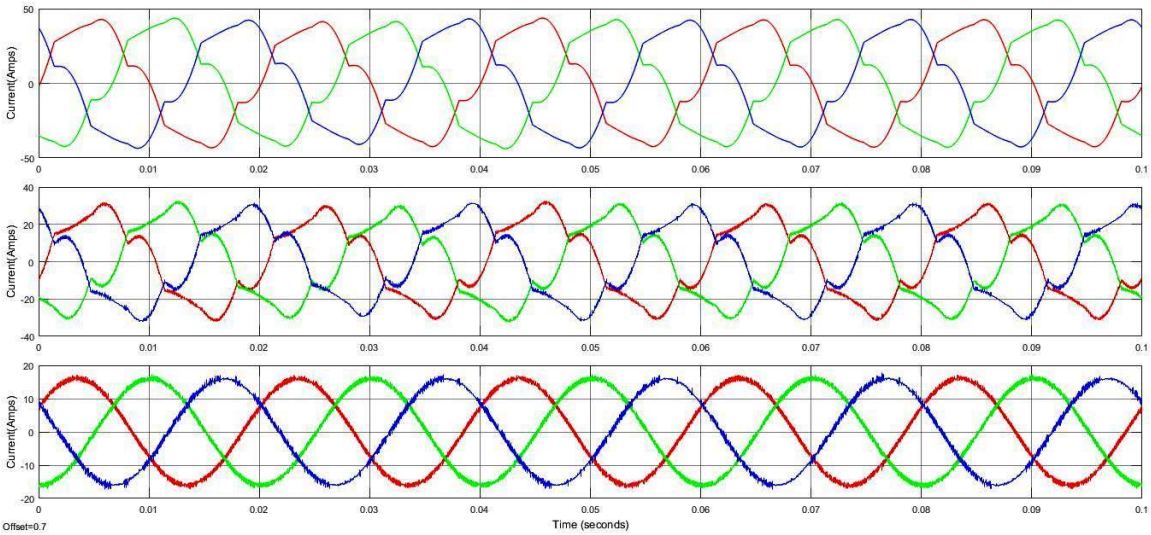

(b) Load current, Injected current, Source current

FIGURE 15. Waveforms of proposed system for case-2.

the solution vector i.e K_p, K_i where, the objective (THD) is minimum.

IV. FUZZY CONTROLLER FOR DC-LINK

The FL-C takes the E and CE, and generates an output representing the required change in current, which is then added with the output of PI-C. The fuzzy variables are denoted by triangular membership functions for error, change in error and the output duty cycle involving PSH, medium positive (PSM), PSL, ZE, NEH, medium negative (NEM) and NEL as in figures [9], [10], [11], and the developed fuzzy IF-THEN rules are given in Table 6.

The rules attempt to maintain the present control setting $i_{dc} = 0$, when both E and CE are zero, and also when E is not zero but approaching the reference value at a satisfactory rate. When E is increasing, these rules appropriately change the control signal (i_{dc}) depending on the magnitude and the sign of E and CE with a view of forcing E towards zero. Here, the matrix rules are created according to the complexity of the control system. In this control application, the control system involved is two input single output type. Rules are formed according to the system requirements. The fuzzy inference system performs an evaluation of the rules, and then, it combines all of the results to forma final output, which is a fuzzy value. The accurateness can be increased by increasing the number of rules at a cost of increased data size and complexity, and a larger execution time of the control system [7].

V. SIMULATION AND RESULTS

The performance of proposed U-PVBS was studied on a grid connected 3-φ AC distribution system. The simulink model

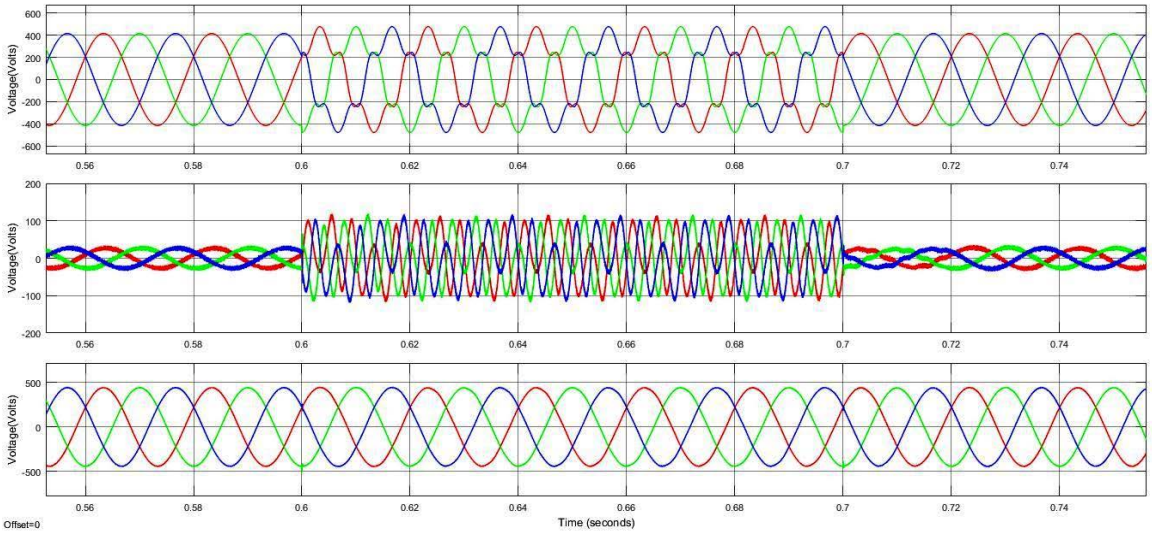

(a) Source voltage, Injected voltage, Load voltage

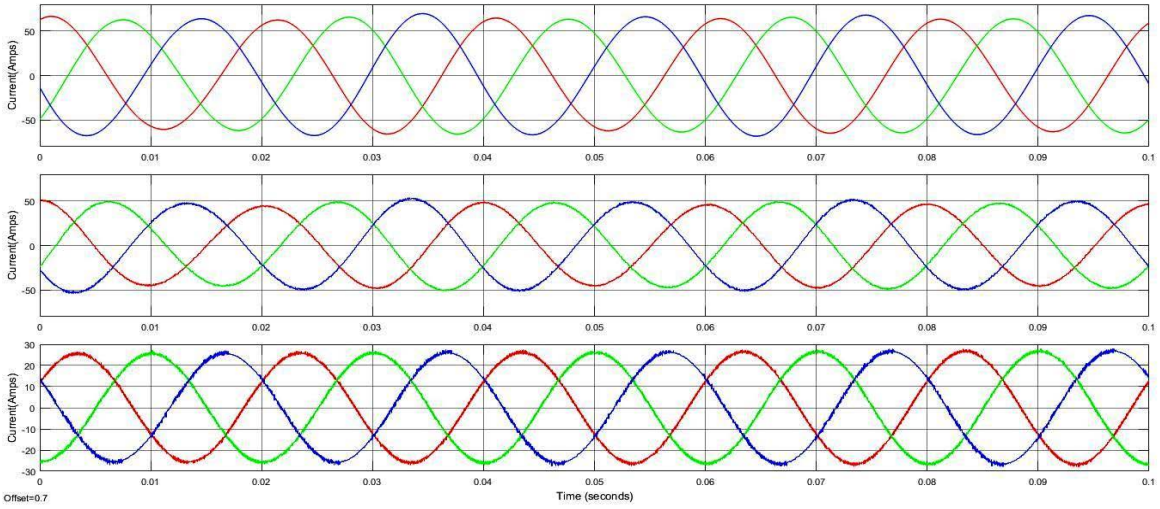

(b) Load current, Injected current, Source current

FIGURE 16. **Waveforms of proposed system for case-3.**

for the U-PVBS with different loads has developed in Matlab-2016a as exhibited in figure 12. The approach has been carried out 20times and the best one has been presented as an optimal solution. Four test cases with the different combinations of nonlinear/unbalanced loads, sag/swell/disturbance, and variation in irradiation are exhibited in Table 7, were considered for analyzing the performance of the U-PVBS. The supply voltage was considered to be balanced for cases 1-3 and unbalanced for case 4. In addition, source voltage sag was considered in case 1, voltage swells in case 2, and large voltage disturbances in case 3 respectively. The results are compared with existing methods PI-C, GA, BBO. The lower/upper bonds for the control variables are in range of [0.0001 100], and the chosen parameters for the SOL along with are given in Table 5. The obtained optimal control parameters by the proposed SLOHC along with existing methods are exhibited in Table 9. The PF is calculated by Eq. (23) for all test cases and comparisons with PI-C, GA, and BBO are given in figure13.

$$Powerfactor = \cos\theta * \frac{1}{\sqrt{1 + THD^2}} \tag{23}$$

where, θ is the angle between voltage, current while it represent the displacement factor. The voltage sag or swell with SLOHC is calculated by Eq. (24)

$$V_{sag/swell} = \frac{V_l - V_S}{V_l} = \frac{V_{se}}{V_l} \tag{24}$$

The voltage injected by the series compensator to compensate voltage sag/swell and disturbance of U-PVBS is given by Eq. (25) [7].

$$V_{se} = V_l - V_S \tag{25}$$

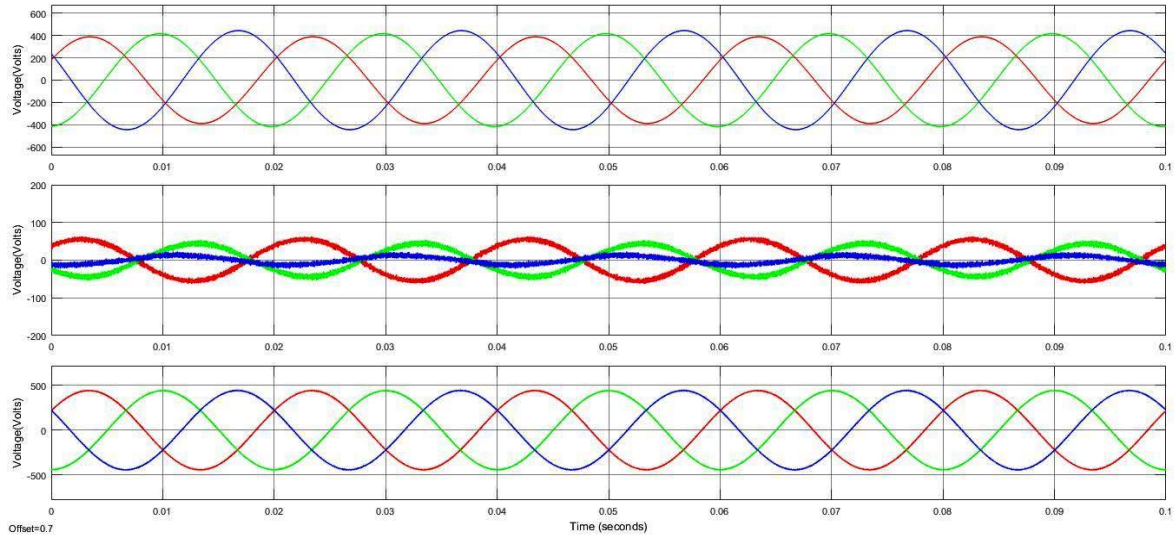

(a) Source voltage, Injected voltage, Load voltage

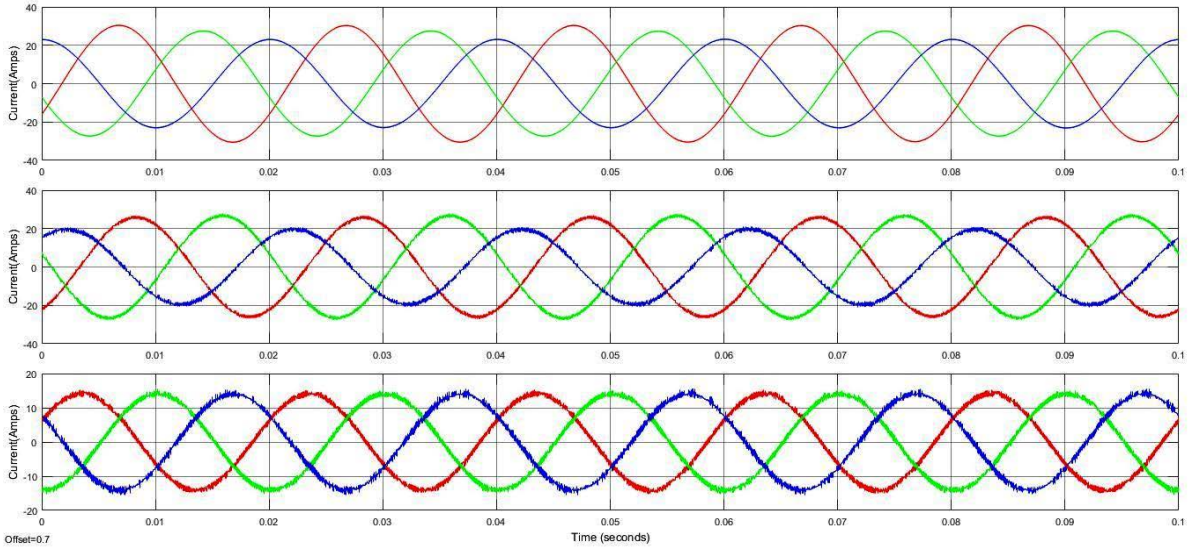

(b) Load current, Injected current, Source current

FIGURE 17. **Waveforms of proposed system for case-4.**

The current injected by the shunt compensator is given by Eq. (26) [7].

$$i_{sh} = i_i - i_S \tag{26}$$

Figure 13 exhibits that the PF of proposed method is much higher that of standard methods and the waveforms of the proposed U-PVBS for the test cases 1-4 are illustrated in Fig. 14-17.

In Table 8, the THD of the proposed method for all case studies was compared with those of the existing real and practical methods as cases that are available in the literature with citations. The reason behind choosing GA and BBO for comparison is GA is one of the standard genetic inspired algorithms while BBO is the study on natural biogeography. BBO has features in common with other biology-based optimization methods, such as GAs and particle swarm optimization (PSO) to show the superiority of the proposed method these two optimizations was chosen.

However, according to the results and comparative analysis it clearly exhibits the superior performance of the proposed method in reducing THD. Figure 13 exhibits that the PF of proposed method is much higher that of standard methods. Selection of the suitable algorithm plays a vital role which mainly depends on the objective function of the optimization problem. Generally, classical techniques give more accurate results but they are time consuming and having some limitations. For faster processing you can select the meta-heuristic algorithms.

In case-1, the source voltage was sagged by 30% during the interval of 0.25-0.35s; the proposed U-PVBS injects

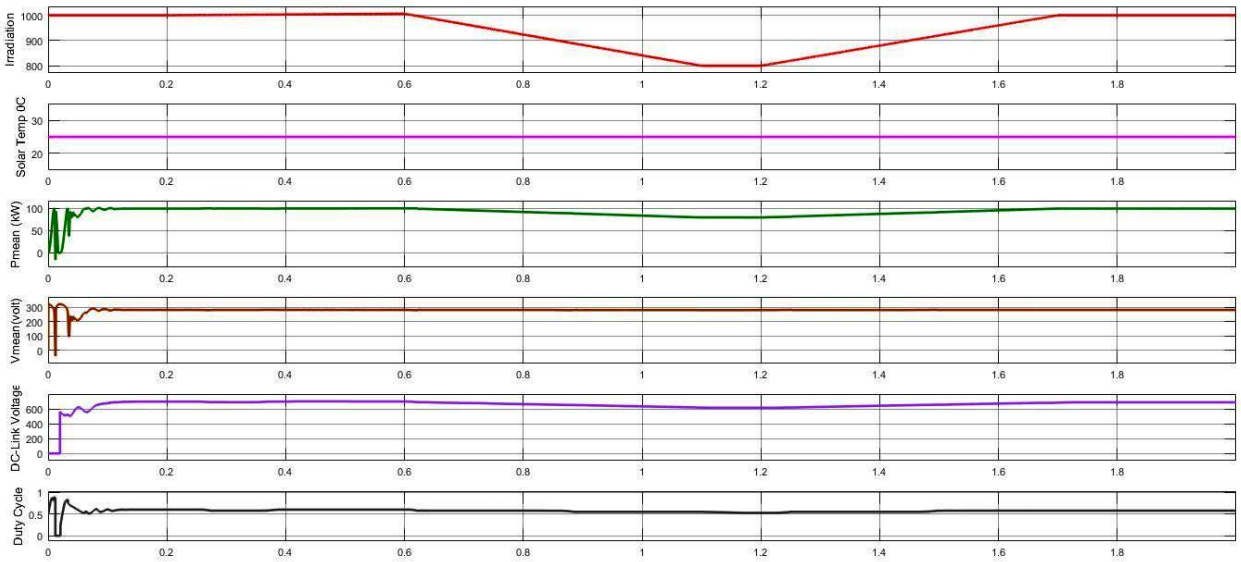

FIGURE 18. Waveforms of Solar irradiation, Temperature, solar output power, solar Voltage, DC-Link voltage, Duty cycle.

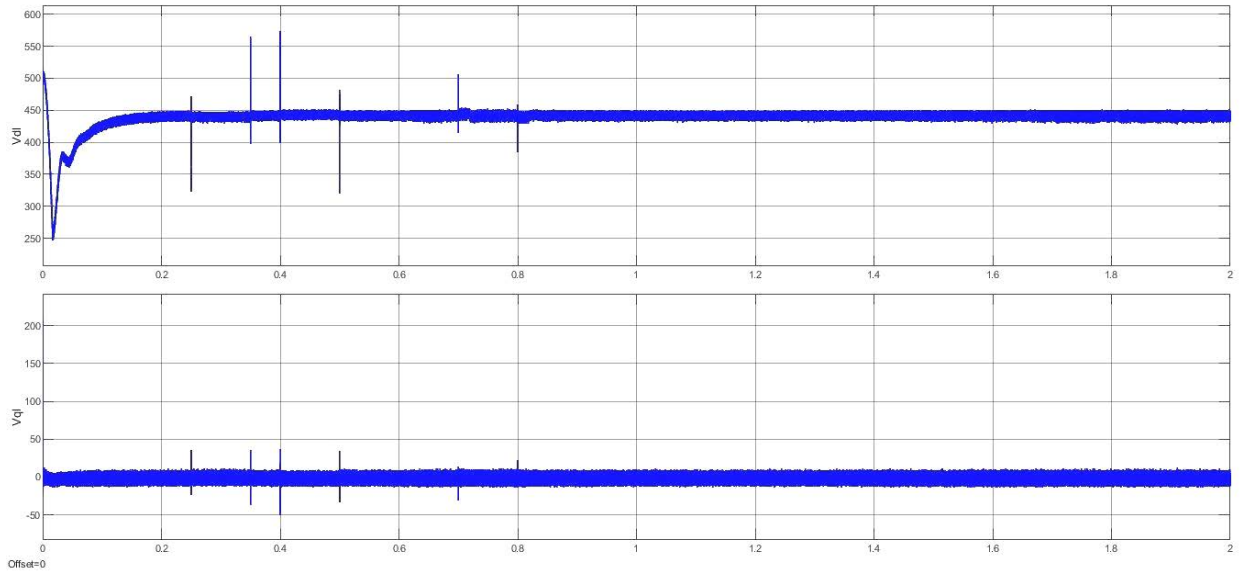

FIGURE 19. Load voltage in d-q frame.

a suitable amount of required voltage to improve the load voltage as shown in figure 14(a). Moreover, the load current was observed to be balanced but non-sinusoidal with the THD of 27.67%, and PF of 0.783 due to the non-linear rectifier load as shown in figure 14(b). It can be seen clearly from figure 14 that the proposed U-PVBS was able to eliminate sag effectively by injecting suitable compensating voltage and improves sinusoidal source current. However, such improvement in current waveforms reflects to the THD and PF values. Therefore, the THD of the load current was reduced from 27.67% to 2.06% and the PF rose from 0.783 to 0.989 by injecting appropriate shunt currents. The Kp, Ki values of shunt and series controllers K_{p_sh}, K_{i_sh}, $K_{p\_se\_d}$, $K_{i\_se\_d}$, $K_{p\_se\_q}$, $K_{i\_se\_q}$ are optimal tuned to 1.0112, 18.0323, 1.0057, 1.01200, 14.0025, 0.0011respectively while satisfying the limits.

In case-2, the voltage swell was introduced from interval 0.4 to 0.5s; the proposed system effectively eliminates it by injecting suitable compensating voltage as shown in figure 15(a). However, always a negligible amount of voltage exits across the series converter during steady state. Here, the load current was observed to be non-sinusoidal but balanced with a THD of 15.89% and a PF of 0.623 due to the non-linear rectifier and motor load connected simultaneously as presented in figure 15(b). It can be seen that the U-PVBS was able to suppress swell successfully and reduce THD from 15.89% to 2.44% thereby boosting up the PF value from 0.623 to 0.985 by injecting suitable shunt currents. The Kp,

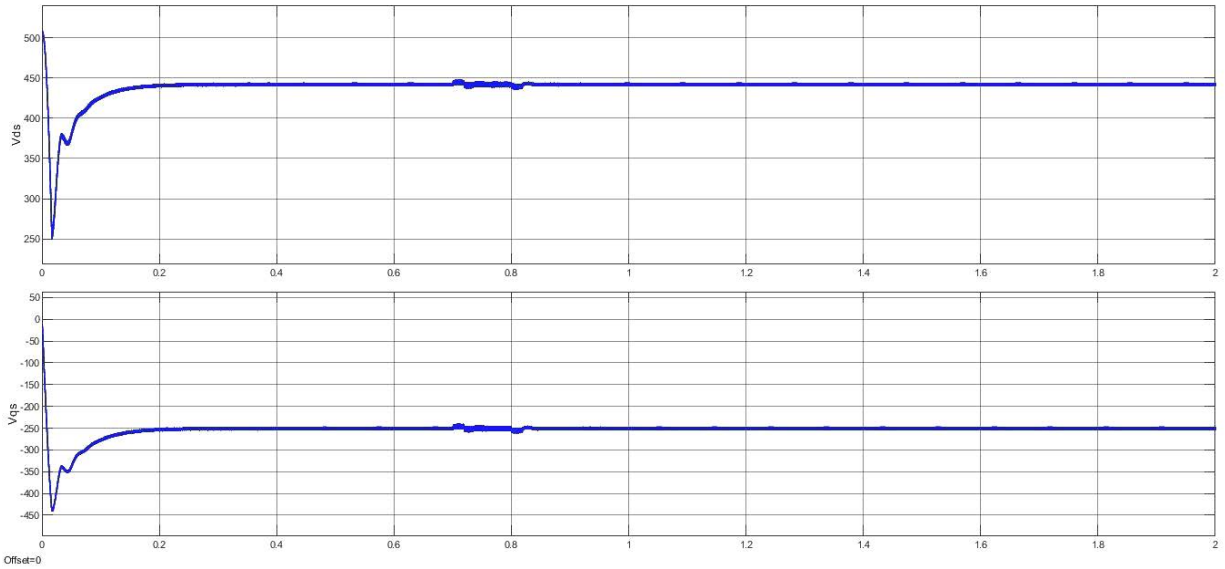

FIGURE 20. Source voltages in d-q frame.

TABLE 9. Comparison of design parameters.

Case	Method	K_{p_sh}	K_{i_sh}	$K_{p\_se\_d}$	$K_{i\_se\_d}$	$K_{p\_se\_q}$	$K_{i\_se\_q}$
1	PI-C	0.712	18.4525	1.2532	15.3123	2.1271	37.1452
	GA	0.00415	0.0171	12.137	1.2581	15.3254	41.3254
	BBO	0.00829	0.0088	0.008	0.1321	0.0141	0.035
	Conv. PI-C [18]	0.507	10.3	--	--	--	--
	ACO-PI-C [18]	0.912	247.93	--	--	--	--
	BF-PI-C [18]	0.843	288.5	--	--	--	--
	PSO [10]	2.1345	10.2581	--	--	--	--
	HSO [10]	3.7151	45.4126	--	--	--	--
	ZN [10]	0.019	0.00042	--	--	--	--
	ICM [10]	0.0455	0.064	--	--	--	--
	ABC [25]	8.2270	0.0020	--	--	--	--
	GSA [25]	9.6325	2.3020	--	--	--	--
	FA [25]	9.2545	1.6580	--	--	--	--
	MFOA [25]	8.8554	1.8569	--	--	--	--
	SLOHC	**1.0112**	**18.0323**	**1.0057**	**1.0120**	**14.0025**	**0.0011**
2	PI-C	6.5201	19.2101	0.3508	13.5721	1.325	10.3214
	GA	2.2112	8.4011	1.2131	58.2464	1.8245	56.378
	BBO	3.0804	5.03	3.2475	9.1308	16.3245	62.289
	SLOHC	**6.0121**	**13.08**	**15.3612**	**4.08**	**2.1087**	**5.6604**
3	PI-C	4.2635	3.6231	44.249	32.6387	2.3651	64.378
	GA	2.241	7.45	16.1332	51.32	12.3657	71.3241
	BBO	12.4965	9.7512	8.32	3.58	3.254	15.378
	SLOHC	**3.023**	**1.32**	**2.2002**	**79.012**	**1.0245**	**54.7854**
4	PI-C	5.0207	0.001	66.9137	94.4397	4.3247	0.1257
	GA	26.6918	19.42	50.7312	0.0132	5.3974	23.478
	BBO	4.1387	0.1001	0.1891	10.1736	3.578	1.3478
	SLOHC	**15.1998**	**0.001**	**6.1940**	**10.001**	**1.3078**	**0.2147**

Ki values of shunt and series controllers are optimally tuned to 6.0121, 13.08, 15.3612, 4.08, 2.1087, 5.6604 respectively.

In case 3 the large voltage disturbance was introduced in the source voltage. Here, the load current was unbalanced and non-sinusoidal with a THD of 33.91% and a PF of 0.668 due to nonlinear and unbalanced loads. It can be seen that the U-PVBS was able to eliminate voltage disturbances very effectively by the suitable compensating voltage and reduce THD from 33.91% to 2.40% thereby raising the PF value from 0.668 to 0.989 in addition to the improving the shape of sinusoidal waveform shown in figure 16(a)-16(b) respectively. The Kp, Ki values of shunt and series controllers are optimally tuned to 3.023, 1.32, 2.2002, 79.012, 1.0245, 54.785 to attain objective function.

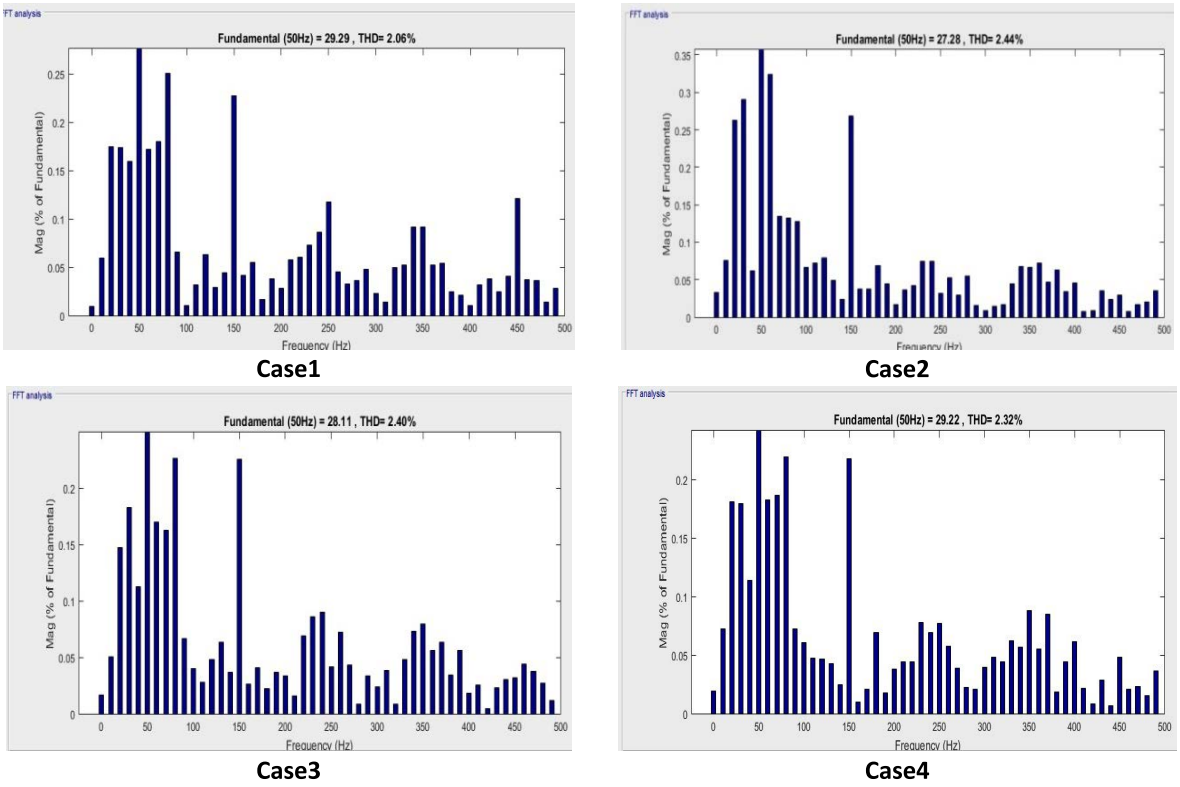

FIGURE 21. THD spectrum for case studies.

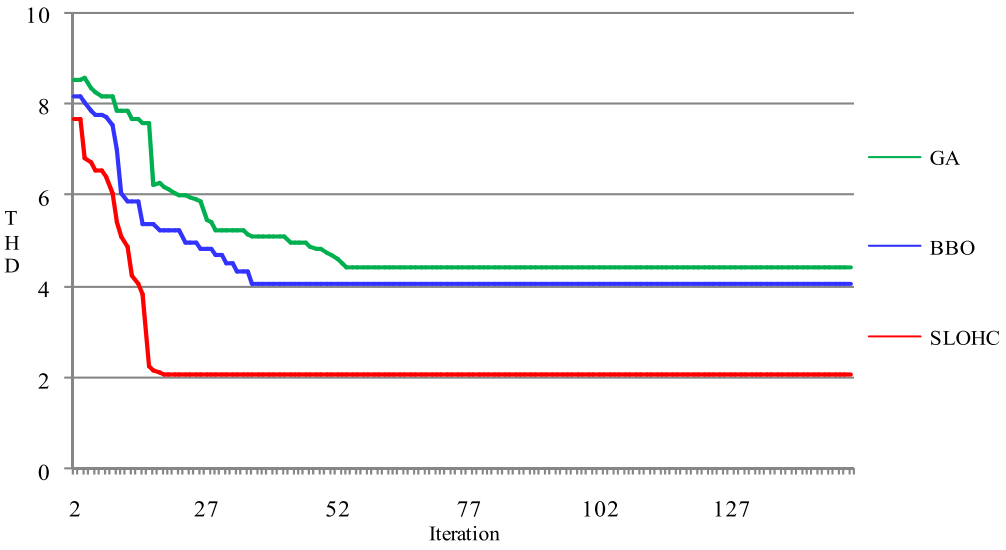

FIGURE 22. Comparison of convergence characteristics for case-1.

In case 4 the unbalanced supply voltage was considered, but proposed U-PVBS effectively provides balanced load voltage as shown in figure 17(a). Here, the load current was seems to be sinusoidal and unbalanced with a THD of 7.33% and a PF of 0.775 figure 17(b). The SLOHC was able to reduce THD from 7.33% to 2.32% and improve PF from 0.775 to 0.999. The performance of the proposed method was tested with solar irradiation variation from 1000 W/m^2 to 800 W/m^2 and from 800 W/m^2 to1000 W/m^2 under the constant 25°c temperature. The Kp, Ki values of shunt and series controllers are optimally tuned to 15.1198, 0.001, 6.194, 10.001, 1.3078, 0.2147 while satisfying the upper and lower limits.

However, from the figure 18 it is clearly understood that the proposed system exhibits its superior performance in maintaining the constant DC-Link voltage during irradiation variation. In addition, to it the output power of PV panel, voltages and duty cycle was also given. The load and source voltages

in d-q frame are shown in figure 19-20. Figure 21 gives the THD spectrum for all four test cases. Figure 22 shows the convergence characteristics of the proposed controller with GA and BBO where it can clearly seen that proposed method converge to an optimal point in a less number of iterations when compared to other methods.

VI. CONCLUSION

A hybrid controller involving FL-C and optimal tuned PI-C was designed for U-PVBS. The controllers of BS and SP were explained in-addition to developing of SOL based PI-C for shunt and series converters and FL-C for DC-Link to regulate and maintain stable DC-link capacitor voltage, eliminating of sags/swells/disturbances in supply voltage, diminishing the THD in load voltage and source current, and boosting the PF. The investigation was carried on four test cases with different combinations of loads, balanced/ unbalanced network voltages, voltage sag/swells/disturbances, and variation on irradiation was exhibited.

The proposed method optimally tunes the K_{i_sh}, K_{p_sh}, $K_{i\_se\_d}$, $K_{p\_se\_d}$, $K_{i\_se\_q}$, $K_{p\_se\_q}$ values to 18.0323, 1.0112, 1.0120, 1.0057, 0.0011, 14.0025 in case-1 in order to satisfy the objective function. Analyzing the THD and PF of the system without U-PVBS the THD value was 27.67% for case1, 15.89% for case2, 33.91%, 7.33% for case3 & 4 and value of PF was 0.783, 0.623, 0.688, and 0.775 for case 1-4 test cases. By implementation of U-PVBS with SLOHC the THD reduces to 2.06%, 2.44%, 2.40%, and 2.32% respectively. It clearly exhibits that the proposed SLOHC was able to lower the THDs within acceptable levels and power factors to almost unity. Moreover, these performances were much better than those of the existing controllers like conventional PI-C, GA, BBO, and controllers that are available in literature. The SLOHC took a smaller time to reach the steady-state dc-link voltage than those of existing methods. This paper presents with an objective of total harmonic distortion for two-level UPQC with simulation results. However, the selective harmonic elimination technique (SHE) can be implemented, and optimal design of two and multi-level UPQC for the microgrid with hard ware can be designed as the future study.

REFERENCES

[1] Y.-W. Wang, M.-C. Wong, and C.-S. Lam, "Historical review of parallel hybrid active power filter for power quality improvement," in *Proc. IEEE Region Conf.*, Nov. 2015, pp. 1–6.

[2] N. G. Hingorani, "Flexible AC Transmission," *IEEE Spectr.*, vol. 30, no. 4, pp. 40–45, Apr. 1993.

[3] S. Devassy and B. Singh, "Design and performance analysis of three-phase solar PV integrated UPQC," in *Proc. IEEE 6th Int. Conf. Power Syst. (ICPS)*, Mar. 2016, pp. 73–81.

[4] P. K. Dash, S. K. Panda, T. H. Lee, J. X. Xu, and A. Routray, "Fuzzy and neural controllers for dynamic systems: An overview," in *Proc. 2nd Int. Conf. Power Electron. Drive Syst.*, 1997, pp. 810–816.

[5] S. Mikkili and A. K. Panda, "RTDS hardware implementation and simulation of SHAF for mitigation of harmonics using p-q control strategy with PI and fuzzy logic controllers," *Frontiers Electr. Electron. Eng.*, vol. 7, no. 4, pp. 427–437, Jun. 2012.

[6] H. C. Lin, "Intelligent neural network-based fast power system harmonic detection," *IEEE Trans. Ind. Electron.*, vol. 54, no. 1, pp. 43–52, Feb. 2007.

[7] S. S. Dheeban and N. B. M. Selvan, "ANFIS-based power quality improvement by photovoltaic integrated UPQC at distribution system," *IETE J. Res.*, vol. 6, no. 2, pp. 1–19, Feb. 2021.

[8] B. Gopal, P. K. Murthy, and G. N. Sreenivas, "Power quality improvement using UPQC integrated with distributed generation network," *Int. J. Elect. Comput. Eng.*, vol. 8, no. 7, pp. 1216–1224, 2014.

[9] G. B. Mohankumar and S. Manoharan, "Performance analysis of multi converter unified power quality conditioner with dual feeder system using fuzzy logic control," *Int. J. Control Autom.*, vol. 8, no. 3, pp. 251–270, Mar. 2015.

[10] S. Mahaboob, S. K. Ajithan, and S. Jayaraman, "Optimal design of shunt active power filter for power quality enhancement using predator-prey based firefly optimization," *Swarm Evol. Comput.*, vol. 44, pp. 522–533, Feb. 2019.

[11] K. Sarker, D. Chatterjee, and S. K. Goswami, "A modified PV-wind-PEMFCS-based hybrid UPQC system with combined DVR/STATCOM operation by harmonic compensation," *Int. J. Model. Simul.*, vol. 41, no. 4, pp. 243–255, Jul. 2021.

[12] V. Vinothkumar and R. Kanimozhi, "Retraction note to: Power flow control and power quality analysis in power distribution system using UPQC based cascaded multi-level inverter with predictive phase dispersion modulation method," *J. Ambient Intell. Humanized Comput.*, vol. 12, pp. 6445–6463, May 2022.

[13] A. Kalair, N. Abas, A. R. Kalair, Z. Saleem, and N. Khan, "Review of harmonic analysis, modeling and mitigation techniques," *Renew. Sustain. Energy Rev.*, vol. 78, pp. 1152–1187, Oct. 2017.

[14] T. S. Saggu, L. Singh, B. Gill, and O. P. Malik, "Effectiveness of UPQC in mitigating harmonics generated by an induction furnace," *Electr. Power Compon. Syst.*, vol. 46, no. 6, pp. 629–636, Apr. 2018.

[15] S. Vinnakoti and V. R. Kota, "Implementation of artificial neural network based controller for a five-level converter based UPQC," *Alexandria Eng. J.*, vol. 57, no. 3, pp. 1475–1488, Sep. 2018.

[16] M. Yavari, S. H. Edjtahed, and S. A. Taher, "A nonlinear controller designs for UPQC in distribution systems," *Alexandria Eng. J.*, vol. 57, no. 4, pp. 3387–3404, 2018.

[17] S. Samal and P. K. Hota, "Design and analysis of solar PV-fuel cell and wind energy based microgrid system for power quality improvement," *Cogent Eng.*, vol. 4, no. 1, pp. 1–21, 2017.

[18] A. Sakthivel, P. Vijayakumar, A. Senthilkumar, L. Lakshminarasimman, and S. Paramasivam, "Experimental investigations on ant colony optimized PI control algorithm for shunt active power filter to improve power quality," *Control Eng. Pract.*, vol. 42, pp. 153–169, Sep. 2015.

[19] V. V. Nagireddy, V. R. Kota, and D. V. A. Kumar, "Hybrid fuzzy back-propagation control scheme for multilevel unified power quality conditioner," *Ain Shams Eng. J.*, vol. 9, no. 4, pp. 2709–2724, Dec. 2018.

[20] K. Srilakshmi, P. R. Babu, Y. Venkatesan, and A. Palanivelu, "Soccer league optimization for load flow analysis of power systems," *Int. J. Numer. Model., Electron. Netw., Devices Fields*, vol. 35, no. 2, pp. 2709–2724, Mar. 2022.

[21] S. J. Alam, S. R. Arya, and R. K. Jana, "Biogeography based optimization strategy for UPQC PI tuning on full order adaptive observer based control," *IET Gener., Transmiss. Distrib.*, vol. 15, no. 2, pp. 279–293, Jan. 2021.

[22] U. K. Renduchintala, C. Pang, K. M. Tatikonda, and L. Yang, "ANFIS-fuzzy logic based UPQC in interconnected microgrid distribution systems: Modeling, simulation and implementation," *J. Eng.*, vol. 21, no. 1, pp. 1–29, 2021.

[23] S. Devassy and B. Singh, "Performance analysis of solar PV array and battery integrated unified power quality conditioner for microgrid systems," *IEEE Trans. Ind. Electron.*, vol. 68, no. 5, pp. 4027–4035, May 2021.

[24] C. Pazhanimuthu and S. Ramesh, "Grid integration of renewable energy sources (RES) for power quality improvement using adaptive fuzzy logic controller based series hybrid active power filter (SHAPF)," *J. Intell. Fuzzy Syst.*, vol. 35, no. 1, pp. 749–766, Jul. 2018.

[25] P. Rajesh, F. H. Shajin, and L. Umasankar, "A novel control scheme for PV/WT/FC/battery to power quality enhancement in micro grid system: A hybrid technique," *Energy Sources A, Recovery, Utilization, Environ. Effects*, vol. 43, no. 3, pp. 1–18, Jul. 2021.

[26] S. S. Dheeban, N. B. S. Muthu, and U. Subramaniam, "Artificial neural network based solar energy integrated unified power quality conditioner," *Energy Sources A, Recovery, Utilization, Environ. Effects*, vol. 43, no. 3, pp. 1–25, May 2021.

[27] F. Nkado, F. Nkado, I. Oladeji, and R. Zamora, "Optimal design and performance analysis of solar PV integrated UPQC for distribution network," *EJECE, Eur. J. Elect. Eng. Comput. Sci.*, vol. 5, no. 5, pp. 1–8, 2021.

[28] S. Gade, R. Agrawal, and R. Munje, "Recent trends in power quality improvement: Review of the unified power quality conditioner," *ECTI Trans. Electr. Eng., Electron., Commun.*, vol. 19, no. 3, pp. 268–288, Oct. 2021.
[29] H. Ahmed and D. Çelik, "Sliding mode based adaptive linear neuron proportional resonant control of Vienna rectifier for performance improvement of electric vehicle charging system," *J. Power Sources*, vol. 542, no. 15, pp. 231–788, 2022.
[30] D. Çelik and M. E. Meral, "A coordinated virtual impedance control scheme for three phase four leg inverters of electric vehicle to grid (V2G)," *Energy*, vol. 246, pp. 123–354, May 2022.
[31] D. Çelik, "Lyapunov based harmonic compensation and charging with three phase shunt active power filter in electrical vehicle applications," *Int. J. Elect. Power Energy Syst.*, vol. 136, pp. 107–564, May 2022.
[32] S. K. Prince, K. P. Panda, and G. Panda, "Kalman filter variant intelligent control for power quality improvement in photovoltaic active power filter system," *Int. Trans. Electr. Energy Syst.*, vol. 30, no. 3, Mar. 2020, Art. no. e12239.
[33] M. Badoni, A. Singh, A. K. Singh, H. Saxena, and R. Kumar, "Grid tied solar PV system with power quality enhancement using adaptive generalized maximum versoria criterion," *CSEE J. Power Energy Syst.*, vol. 12, no. 4, pp. 1–10, Jun. 2021.
[34] M. Badoni, A. Singh, and B. Singh, "Power quality enhancement using Euclidean direction search based control technique," *IEEE Trans. Ind. Electron.*, vol. 67, no. 3, pp. 2231–2240, Mar. 2020.

KOGANTI SRILAKSHMI received the B.Tech. degree in EEE from the Princeton College of Engineering and Technology, Hyderabad, affiliated to JNTU, Hyderabad, Telangana, in 2006, and the M.Tech. degree in EPE from the Sreenidhi Institute of Science and Technology, Hyderabad, in 2010. She is currently pursuing the Ph.D. degree with the Department of Electrical Engineering, Annamalai University, Tamil Nadu, India. She is also working as an Assistant Professor with the EEE Department, Sreenidhi Institute of Science and Technology. She has published 16 reputed international journals. Her research interests include optimal power flow, FACTS, power quality, meta heuristic optimization techniques, and soft computing application in power system engineering.

NAKKA SRINIVAS received the Bachelor of Technology degree in electrical and electronics engineering from the Sri Vasavi Engineering College, Tadepalligudem, India, in 2007, and the Master of Technology degree in energy systems from JNTU, Hyderabad, Andhra Pradesh, India, in 2012. He is currently pursuing the Ph.D. degree in EEE with Annamalai University, Tamil Nadu. He is also working as an Assistant Professor at the Department of EEE, Vardhaman College of Engineering, Hyderabad. He has 14 years of teaching experience in electrical and electronics engineering. He has published seven international journal articles, one national conference, and one international conference paper. His research and teaching interests include electrical machines, power systems, and power quality improvement.

PRAVEEN KUMAR BALACHANDRAN (Senior Member, IEEE) received the B.E. degree in electrical and electronics engineering and the M.E. and Ph.D. degrees in power systems engineering from Anna University, Chennai, India, in 2014, 2016, and 2019, respectively. He is currently working as an Associate Professor with the Department of Electrical and Electronics Engineering, Vardhaman College of Engineering, Hyderabad, India. He has published various research papers in reputed journals. He has filed ten patents and he has three book chapters in his credential. He is also an Active Member of IEEE Power and Energy Society and in five more professional bodies. He is acting as a guest editor for the journals from MDPI, Wiley, Hindawi, and River publishers. His current research interests include solar photovoltaics, solar still, and renewable energy systems.

JONNALA GANESH PRASAD REDDY received the B.Tech. degree in EEE from the Shri Dharmasthala Manjunatheshwara College of Engineering and Technology, Dharwad, affiliated to Karnataka University, Karnataka, in 1998, the M.Tech. degree in HVE from Jawaharlal Nehru Technological University, Kakinada, Andhra Pradesh, in 2005, and the Ph.D. degree in electrical and electronics engineering from Jawaharlal Nehru Technological University Hyderabad, Telangana, in April 2021. He has published several research papers in Scopus indexed journals. His research interests include FACTS, power quality, and different optimization techniques.

SRAVANTHY GADDAMEEDHI received the B.Tech. degree in electrical and electronics engineering and the M.Tech. degree in power electronics from JNTU Hyderabad, Telangana, India, in 2008 and 2010, respectively. She is currently pursuing the Ph.D. degree with the Department of Electrical Engineering, Osmania University, Hyderabad, Telangana. She is also working as an Assistant Professor with the Department of Electrical and Electronics Engineering, Sreenidhi Institute of Science and Technology, Hyderabad. Her research interests include power electronics, electrical drives and control, and FACTS.

NAGARAJU VALLURI received the B.Tech. degree in ECE from JNTU Hyderabad, affiliated to Adilabad, Telangana, in 2008, and the M.Tech. degree in MRE from Andhra University, Visakhapatnam, in 2010. He is currently pursuing the Ph.D. degree with the Department of ECE, Bharat University, Chennai, Tamil Nadu, India. He is also working as an Assistant Professor with the ECE Department, Sreenidhi Institute of Science and Technology, Hyderabad, Telangana.

SHITHARTH SELVARAJAN (Senior Member, IEEE) received the B.Tech. degree in information technology from the KGiSL Institute of Technology, Coimbatore, India, affiliated to Anna University, Chennai, India, in 2012, and the M.E. and Ph.D. degrees in computer science and engineering from Anna University. He is currently working as an Associate Professor at Kebri Dahar University, Ethiopia. He has published more than ten international journals along with 12 international and national conferences. He has even published three patents in IPR. He is also an Active Member of IEEE Computer Society and in five more professional bodies. His current research interests include cyber security, critical infrastructure and systems, and network security and ethical hacking. He is an active researcher, a reviewer, and an editor for many international journals.